Journal of Archaeological Science: Reports

ISSN 2352-409X

DOI: 10.1016/j.jasrep.2020.102648

Submerged and reused: an archaeometric approach to the Early Modern ceramics from Aveiro (Portugal)

Uxue Sanchez-Garmendia[1]*, Patricia Carvalho[2], José Bettencourt[2], Ricardo C. Silva[3], Gorka Arana[4] and Javier G. Iñañez[5]

[1]*GPAC, Built Heritage Research Group. Department of Analytical Chemistry, Faculty of Science and Technology, University of the Basque Country UPV/EHU, Leioa, Basque Country, Spain. E-mail: uxue.sanchez@ehu.eus*

[2]*CHAM FCSH, Universidade NOVA de Lisboa, Av. de Berna, 26C, Edifício I&D, 1069-061 Lisboa, Portugal. E-mails: patriciasanchescarvalho@gmail.com; jbettencourt.cham@gmail.com*

[3]*Faculty of Arts and Humanities. University of Coimbra, Portugal, Palácio de Sub-Ripas, 3000-395 Coimbra, Portugal. E-mail: rcosteiradasilva@gmail.com*

[4]*IBeA, Department of Analytical Chemistry, Faculty of Science and Technology, University of the Basque Country UPV/EHU, Bilbao, Basque Country, Spain. E-mail: gorka.arana@ehu.eus*

[5]*GPAC, Built Heritage Research Group, Faculty of Arts, University of the Basque Country UPV/EHU, Vitoria-Gasteiz, Basque Country, Spain. E-mail: javier.inanez@ehu.eus*

**Corresponding author*

Aveiro, a city located in northern Portugal that lies next to the Atlantic Ocean, has a long potting tradition. Indeed, during the 15th-17th centuries, this region played an important role in the maritime trade between the north of Europe, the Iberian Peninsula and the Atlantic. Historical records reflect regular trade contacts between ship-owners and masters of Aveiro with English, Irish, Flemish, Galician and Basque entrepreneurs, in Europe and overseas.

The archaeological research carried out on the Ria de Aveiro A (RAVA) shipwreck collection (16th - beginning 17th centuries), revealed a large amount of ceramics as cargo, tentatively produced in Aveiro Region. That was compared to a collection from *Santo António* church, in Aveiro, which includes ceramics used to fill the upper choir dome, with an exact chronology (1524), also manufactured in Aveiro. Such set of pottery enabled the establishment of a typology divided in three groups, used in everyday life at that time in Aveiro (tableware, long-distance storage and transportation and sugar moulds) and combining red and black pastes and shiny and matte black finished surfaces.

With a view to characterize and to assess the provenance of local or regional origin of this Post-Medieval pottery assemblage from the two sites, an archaeometric approach of 25 unglazed ceramics showing red and black pastes has been performed. In this way, chemical and mineralogical analyses have been carried out by Inductively Coupled Plasma-Mass Spectrometry (ICP-MS) and X-Ray Diffraction (XRD), and microstructural analysis by Scanning Electron Microscopy-Energy Dispersive Spectrometry (SEM-EDS) analytical techniques. The results show that ceramics from RAVA have a compatible chemical fingerprint with those from the church, forming the A-1 local production

reference group. Moreover, the A-1 reference group has been further assessed by comparing against the main reference groups from the Iberian Peninsula.

Keywords: pottery; Aveiro; shipwreck; archaeometric; ICP-MS; DRX; SEM-EDS

1. Introduction

Aveiro, a city located in the west of the Iberian Peninsula, in Portugal, lies next to a large lagoon area called Ria de Aveiro (Figure 1). Separated from the Atlantic Ocean by a line of dunes more than 50 km long, the lagoon influenced the life of the inhabitants from Medieval times to the Early Modern age; and settlements, which were strongly related to maritime activities and trading, combined agriculture with salt production and fishing. As a consequence, it became an important maritime port. Moreover, these economic activities -often seasonal and complementary- marked the landscape of the lagoon (Alves et al., 2001; Amorim, 2011; Carvalho et al., 2014).

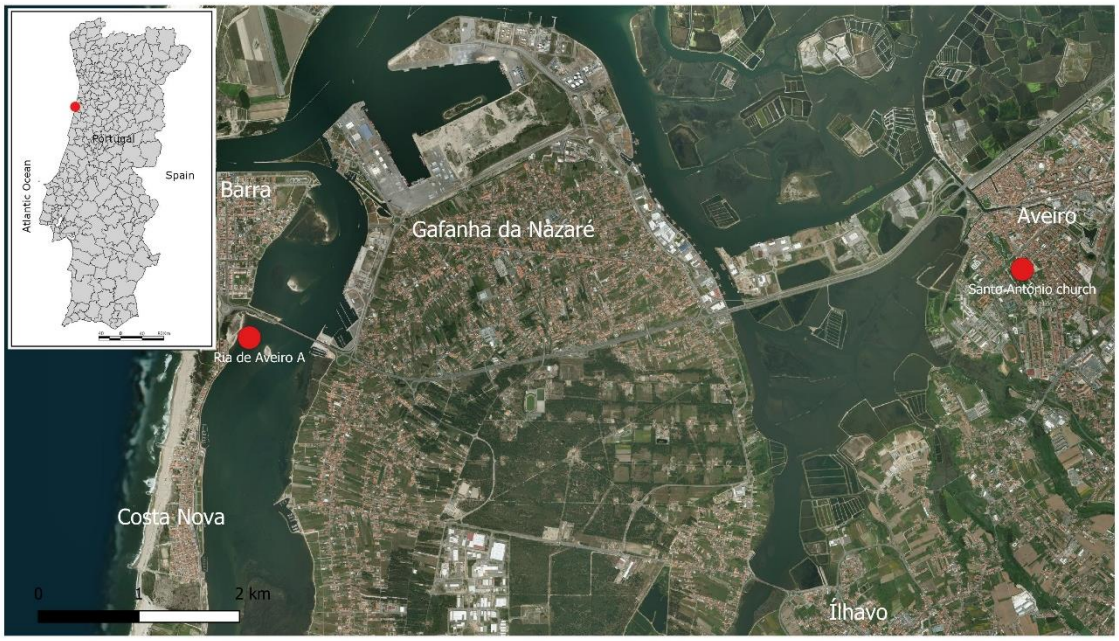

Figure 1. The location of Aveiro in the map of Portugal (red circle) and the location of Ria de Aveiro A (RAVA) and *Santo António* church in the principal map (red circles).

Nevertheless, Aveiro not only was famous because of its maritime activities and trading; the city was, and nowadays still is, a traditional ceramic production region, with high variety and availability of clay reserves. The chemical and mineralogical properties of these clays led to their use as a raw material for the ceramic manufacturing. Pottery production increased in the early 16th century, due to the growth of the city and the maritime trade, which demanded pottery to supply ships and commerce (Barbosa et al., 2009; Bettencourt and Carvalho, 2007-2008; Carvalho and Bettencourt, 2012).

Aveiro featured both red and black coarsewares, showing similar paste features. The red ware assemblage, fired in an oxidising environment, is composed of pieces of an orangey to red colours, with darker grey surfaces. Many exemplars have different shades and even black stains on the outer surfaces as a result of variations in the firing environment and kiln temperature. A small percentage of the assemblage is represented by black vessels, fired in a reductive environment, with pastes of grey and black tones, sometimes with a visible metallic shine. The macro-visual

observation revealed a very fine and hard paste, and the two groups show the same inclusions: quartz and mica, fine to medium grained, well distributed throughout the matrix. Mica is more abundant, being very visible on the exterior surfaces. Most of the vessels may have received some surface treatments which consisted mainly on smoothing the surfaces, in some cases after the application of a slip of the same colour as the paste, but slightly darker (Bettencourt and Carvalho, 2007-2008; Carvalho and Bettencourt, 2012).

Those ceramics can be classified in different groups, such as for domestic use, like tableware (e.g. cups, bowls, jars), kitchenware (cooking pots) and personal hygiene (bacins); long-distance storage and transportation (e.g. olive jars); and sugar moulds (*formas de açúcar*) (Figure 2).

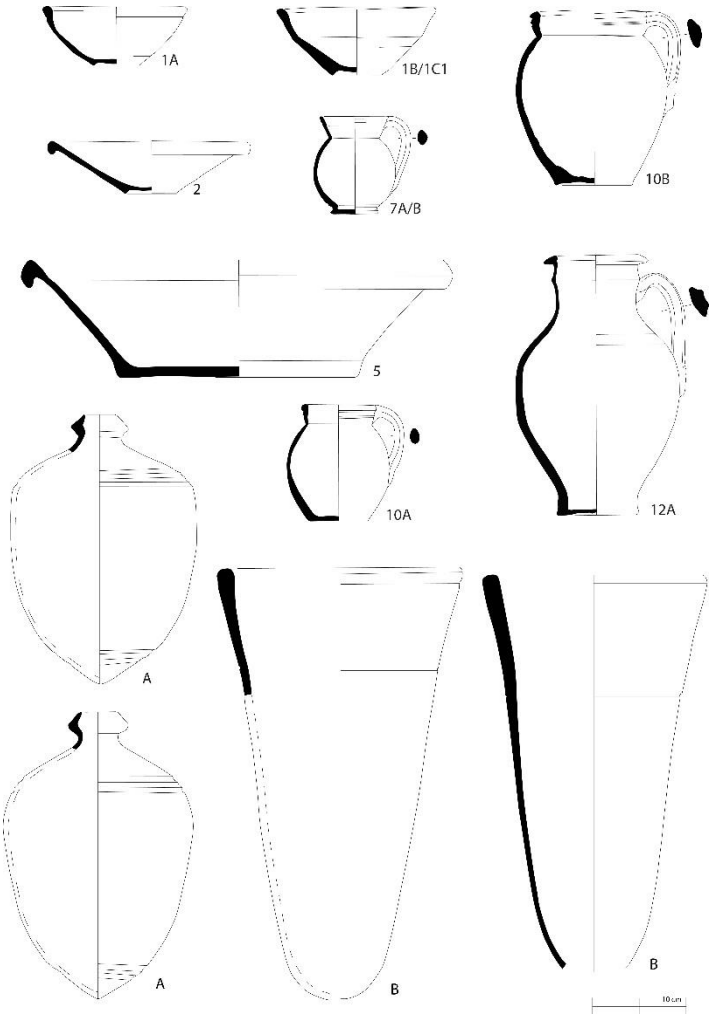

Figure 2. Main pottery forms: A – olive jars; B – sugar moulds; 1A/1B/1C – bowls; 2 – plate; 5 – basins; 7A/B – mugs; 10A/B – cooking pots; 12A – jar.

Sugar moulds were essential for the sugar production process. They are conical moulds, with a hole in their top. Nowadays, it is common to find discarded pieces as a constituent element of the wall of the old buildings in the old town of the city (Bettencourt and Carvalho, 2007-2008; Morgado et al., 2012). In recent years, sugar moulds, as well as pottery with different typologies from Aveiro, have been identified in international locations. According to Silva (2018), Aveiro was, probably, since the 16th century, the main producer and supplier of sugar moulds in the sugar production areas of the Kingdom of Portugal, such as Madeira, Azores, Cape Verde and had a

strong impact in other markets like Canaries. Ceramics from Aveiro were also found in England and Newfoundland. All these facts are evidence of the Atlantic and transatlantic trade flows during the Medieval, Post-Medieval and Modern Periods. Portugal was certainly a major consumer of English-caught Newfoundland cod (Bettencourt and Carvalho, 2007-2008; Carvalho and Bettencourt, 2012; Newstead, 2014; Silva, 2018).

On the other hand, the traditional salt production in the region is well known since the 10th century and the production was increased after the 13th century, due to the constant salinity levels of the lagoon water as well as the favourable landscape and environmental conditions. In fact, several maps show the salt production locations in the lagoon, such as the map made by the Dutch cartographer Lucas Janszoon Waghenaer in 1584 (Figure 3). In this way, Aveiro also played an important role in the supply of salt since the Middle Ages, not only to North-western Europe (England, the Low Countries, Finland and Sweden), but also to the north of Spain, in particular Galicia and Asturias, as well as to the Dutch market, during the 16th and 17th centuries (Amorim, 2019; Antunes, 2008a). Salt was used in manufacturing and preservation of food and hides. Fishing and other activities were heavily dependent on this by-product of the sea (Antunes, 2008b).

Figure 3. Sea map of Portugal made by the Dutch cartographer Lucas Janszoon Waghenaer in 1584. The salt production centers of Aveiro could be seen in the fourth river starting to the left. *[Title: Gedaente en vodoeninge vant Landt van Portugal; from: Mariner's Mirror (T'eerste deel vande Spieghel der zeevaerdt, van de navigatie der Westersche zee, innehoudende alle de custen van Vranckrijck, Spaingen ende 't principaelste deel van Engelandt, in diversche zee caerten begrepen", Leiden, Christoffel Plantijn, 1584). Source: University of Texas at Arlington Libraries]*.

The Atlantic distribution of the Aveiro ceramics is documented, in addition to the discovery of Aveiro wares in other localities, thanks to a diverse underwater archaeological record, with nearly a dozen archaeological sites (Carvalho et al., 2014). Some of the examples belong to the archaeological sites called Ria de Aveiro

A, B and C. In the two latter places, a large assemblage of Aveiro ceramics as well as several artefacts related to maritime activities were discovered, suggesting that Aveiro was connected to the routes with the North and the South of Europe since the Middle Ages (Bettencourt, 2009; Carvalho et al., 2014). Moreover, the former case, in which this work will focus on, corresponds to a shipwreck. Ria de Aveiro A (RAVA) was discovered in the Aveiro lagoon (Ílhavo) in 1992. The site preserved the aft end of a small wooden vessel, ca. 18-meter-long ship of Ibero-Atlantic tradition, which transported a coarseware cargo. The cargo was located in the hold of the ship, and the ceramics were protected by a dunnage "mattress" about 200 mm thick, made of interwoven sticks, undergrowth, straw, mats and pine needles (Alves et al., 2001). Carbon-14 analysis conducted at an initial research stage, attributed the context to a chronology from mid-15th century (Alves et al., 2001), but the excavation and study of the ceramic cargo indicates a more recent date, from early modern period, 16th or beginning of the 17th centuries (Carvalho and Bettencourt, 2012). RAVA was interpreted as containing a local ceramics cargo destined to be sold in markets outside the lagoon, but the final destination could not been defined. The size of the cargo and the archaeological context suggest, however, a port located in Portugal as the most probable destination (Bettencourt and Carvalho, 2007-2008).

The large number of recovered ceramic pieces allowed the establishment of a typology with the shapes used in everyday life at that time. Some big ceramics, such as large pots, were carrying smaller pots inside them. Similar ceramics were found in Portugal, particularly in the North (Viana do Castelo, Porto, Coimbra), but also in the Atlantic, in places like Azores, Madeira, Newfoundland, in sites related to seasonal fishing settlement, or on England contexts (Alves et al., 2001; Bettencourt and Carvalho, 2007-2008; Carvalho and Bettencourt, 2012). It should also be noted that several pieces of evidence indicative of a fire on board were documented. These are visible in a set of ceramics, which are burnt, deformed and vitrified (Carvalho and Bettencourt, 2012). Since the ceramics were located in the hold of the ship and they were protected, the firing environment produced around the ceramics could have been a reducing environment.

The present work also focuses on the ceramics recovered in a terrestrial environment, specifically in the filling of the upper choir dome of *Santo António* church in Aveiro. It is estimated to have around 90 pieces of different typologies. The primitive Franciscan convent of *Santo António*, of which only the church and part of the cloister remains, was founded in 1524. It was classified as a National Monument. The use of ceramics in the construction of domes is a peculiar technique of remote origin, probably Roman, which was developed in the Christian Medieval Era. After cleaning the surface remains, it was discovered that the ceramics were methodically placed and surrounded by very fine and loose clay soil. The conditions and context of finding, allowed to assign this lot to a precise chronology (1524). As many of them had manufacturing defects, it is generally assumed that ceramics reused in these contexts were of local production. There was a predominance of red and unglazed earthenware, although some big black cooking pots were also recovered. In addition to the assemblage of household ceramics and sugar moulds already well known in Aveiro, the finding of a group of several olive jars (*anforetas/botijas*) was remarkable because they constituted the main part of the retrieved collection in the church. One of the most characteristic aspects of the olive jars is the distinctive exterior surface treatment by the white slip. This slip is not uniform and does not cover the entire pieces (Silva, 2018).

Regarding the archaeometric analyses of the ceramic materials from Aveiro and surroundings, few studies have been carried out. Among them, the archaeometric investigation by Alves and collaborators (1998), concerning the ceramics recovered in the ship of Ria de Aveiro A, should be noted. In their research, Alves and colleagues catalogued those ceramics as local products after comparing them with the ceramics recovered in *Bairro das Olarias* (Aveiro) and *Casa do Infante* (Porto) by means of X-Ray Fluorescence (XRF). The authors additionally have identified, by XRD, the iron oxide as the common colouring agent, giving different colours (red, brown, grey and black) depending on the oxidation state of the iron. Other relevant study includes the one carried out by Sousa and collaborators (2005). Sousa and colleagues characterized sugar moulds exhumed in Machico (Madeira Island) concluding that these ceramics could have been produced in Aveiro. Additionally, Vieira and collaborators (2013) compared the spectroscopic data obtained by different techniques, such as micro-Raman, from Portuguese faience production from *Mata da Machada* (South of Lisbon) and tin-lead glazed shards found in a medieval house in Aveiro. The obtained results indicate a similarity in the micro-Raman spectrum in their glaze and clays (Vieira et. al., 2013). Recently, Iñañez and collaborators (2020) suggested a probable Aveiro provenance for two unglazed red pots recovered in the shipwreck Angra D (Terceira Island, Azores archipelago), after their archaeometric study.

With a view to characterize and to assess the provenance of local or regional origin of the Post-Medieval pottery assemblage, an archaeometric approach of 25 unglazed ceramics from RAVA and the church showing red or black pastes has been performed. In this way, chemical, mineralogical and microstructural analysis by Inductively Coupled Plasma-Mass Spectrometry (ICP-MS), X-Ray Diffraction (XRD) and Scanning Electron Microscopy coupled to an energy dispersive X-ray analyzer (SEM-EDS) have been carried out. Moreover, their provenance has been further assessed by comparing them with well-known archaeometric reference groups from the main production centres of the Iberian Peninsula (Buxeda i Garrigós et al., 2015; Calparsoro et al., 2019; Iñañez et al., 2008; Iñañez et al., 2009; Sanchez-Garmendia et al., 2020) shedding light on the local consumption patterns and Atlantic and transatlantic trade during the Medieval, Post-Medieval and Modern Periods.

2. Materials and methods

2.1. The ceramic wares

The group of household ceramics (AVR001, AVR002, AVR003, AVR004, AVR005, AVR006, AVR007, AVR008, AVR009, AVR010, AVR011, AVR012, AVR013, AVR014, AVR015, AVR016, AVR022, AVR023, AVR024, AVR025 and AVR026) corresponds to red and black unglazed pottery production, and all ceramics are wheel-made evidenced by concentric marks and lines in their surfaces (Figure 4). There is a predominance of red earthenware, with variations in the colour of the pastes between red-orange and beige. The pastes of this red earthenware are compact, medium hard and with laminar aspect, either purified or with the inclusion of small and medium non-plastic elements (essentially quartz, calcite and mica), well distributed throughout the matrix. The black pastes are similar to the previous ones, distinguished only by the reducing cooking

environment. Among these ceramics, AVR003 and AVR005 are the most uncommon ceramics. The former shows a two-coloured surface and a black paste, whereas the latter is composed by two ceramic shards stuck together (Figure 4). Additionally, there are three pieces of sugar moulds (AVR018, AVR019 and AVR020) (Figure 4). These are distinguished by compact pastes, a sandy texture, light orange colour and little purification, with poorly distributed abundant small-medium non-plastic elements (like quartz grains, mica and small, dark-coloured ferruginous particles) and their surfaces are black matte. Finally, the specific group of containers intended for long-distance storage and transportation is formed by an olive jar (AVR017) (Figure 4). The orange, fine and purified paste differentiates the manufacture of the olive jars. Its surface is not glazed; however, it shows the distinctive exterior surface treatment by the white slip.

The finish of some black ceramics of this assemblage is also worthy of note: four ceramics show a black shiny metallic surface (AVR003, AVR005, AVR015 and AVR016), whereas eight show a black matte one (AVR001, AVR002, AVR012, AVR018, AVR019, AVR020, AVR022 and AVR025) (Figure 4). Regarding the evidence of the firing produced in the ship, AVR005 seems to be totally burnt, showing black pastes and vitrified surfaces. Another shard showing evidence of fire on its surfaces is AVR013. This information is summarized in Table 1.

Figure 4. 25 unglazed red and black pieces unearthed in Ria de Aveiro A and in *Santo António* church, showing red and black pastes and surfaces.

ANID	ARCHAEOLOGICAL SITE	FORM	PASTE	SURFACE
AVR001	RAVA	Basin (*alguidar*)	Beige	Black matte
AVR002	RAVA	Basin (*alguidar*)	Black	Black matte
AVR003	RAVA	Plate (*prato*)	Black	Shiny black and beige
AVR004	RAVA	Mug (*púcaro*)	Beige	Beige
AVR005	RAVA	Storage jar (*talha*)	Black	Shiny black
AVR006	RAVA	Bowl (*tigela*)	Red	Red
AVR007	RAVA	Bowl (*tigela*)	Red	Red
AVR008	RAVA	Basin (*alguidar*)	Beige	Beige
AVR009	RAVA	Bowl (*tigela*)	Beige	Beige
AVR010	RAVA	Mug (*púcaro*)	Red	Red

AVR011	RAVA	Mug (*púcaro*)	Red	Red
AVR012	RAVA	Jar (*cântaro*)	Red	Black matte
AVR013	RAVA	Basin (*alguidar*)	Red	Red and black matte
AVR014	RAVA	Basin (*alguidar*)	Red	Red
AVR015	RAVA	Plate (*prato*)	Black	Shiny black
AVR016	RAVA	Plate (*prato*)	Dark red	Shiny black
AVR017	Church	Olive jar (*anforeta/botija*)	Red	White
AVR018	Church	Sugar mould (*forma de acúcar*)	Red	Black matte
AVR019	Church	Sugar mould (*forma de acúcar*)	Red	Black matte
AVR020	Church	Sugar mould (*forma de acúcar*)	Red	Black matte
AVR022	Church	Cooking pot (*panela*)	Red	Black matte
AVR023	Church	Bowl (*tigela*)	Red	Red
AVR024	Church	Jar (*cântaro*)	Red	Red
AVR025	Church	Jar (*cântaro*)	Red	Black matte
AVR026	Church	Mug (*púcaro*)	Red	Red

Table 1. Analytical Identification (ANID), archaeological site, form and the colour of the pastes and surfaces of the 25 ceramics from RAVA and *Santo António* church.

2.1. Methodology

The set of ceramics (n= 25) was characterized by a multi-analytical approach. Inductively Coupled Plasma-Mass Spectrometry (ICP-MS) and X-Ray Diffraction (XRD) have been carried out for the chemical and mineralogical analyses. In addition, microstructural characterization, and assessment of the extent of vitrification, alterations and contaminations of a subsample out of the shards (n= 16) have been also studied by Scanning Electron Microscopy-Energy Dispersive Spectrometry (SEM-EDS).

2.1.1. Inductively Coupled Plasma-Mass Spectrometry (ICP-MS)

These analyses were performed with a Nexion 300 ICP-MS (Perkin Elmer), provided with an Oneneb pneumatic concentric nebulizer, cyclonic spray chamber and standard nickel cones. Prior to the analyses, the ceramic shards followed a fusion sample treatment as in Sanchez-Garmendia and collaborators (2020), based on the method optimized by García de Madinabeitia and collaborators (2008).

The solutions obtained from the fusion of each ceramic were then treated inside a class 100 clean room, following the methodology described in detail in the study carried out by Sanchez-Garmendia and collaborators (2020). The difference of the present method with the method followed by those authors is that different weights of the Certified Reference Materials used as standards were treated to get solutions of different concentrations in order to obtain external calibrations with wider concentration ranges. First, the solutions were diluted gravimetrically 200 times in a 1 % HNO_3 solution. 10 g of dilution were prepared for each primary solution. The internal standards solution (In) was prepared from 1000 μg/ml stock solutions of Alfa Aesar using Milli-Q quality water for their dilution. Argon was

used as carrier gas in the ICP-MS measurements. In total, 42 elements and compounds were measured: Al_2O_3, Ba, CaO, Ce, Co, Cr, Cs, Cu, Dy, Er, Eu, Fe2O3, Gd, Hf, Ho, K_2O, La, Lu, MgO, MnO, Na_2O, Nb, Nd, Ni, P_2O_5, Pb, Pr, Rb, SiO_2, Sm, Sn, Sr, Ta, Tb, Th, TiO_2, Tm, U, V, Yb, Zn and Zr. The experimental conditions and sample introduction of the ICP-MS are collected in the study carried out by Sanchez-Garmendia and collaborators (2020).

2.1.1.1. Data interpretation

The chemical results have been treated by a chemometric procedure in order to test the similarity of ceramics and subsequently their hypothetical provenance in accordance with the provenance postulate (Weigand et al., 1977). This treatment has followed a statistical procedure following observations on compositional data by Aitchison (1982; 2008), Buxeda (1999) and Buxeda and Kilikoglou (2003). The software employed for all the transformations, statistical analyses and data visualization was R (Core Team 2019). The routines employed are published in a reproducible manner elsewhere (Calparsoro, 2018).

On the one hand, a logarithmic transformation was applied and the comparisons between individuals were performed after dividing all the chemical components by a selected component. In the present work, as a Hierarchical Clustering Analysis (HCA) has been represented, the divisor used was the geometric mean (centered log ratio transformation or clr) and the squared Euclidean distance was graphically represented using the centroid agglomerative algorithm. Therefore, this approach overcomes the problem of the compositional data called “close to unit sum”, when data necessarily sums 100 %. It is important to highlight that the use of logarithms not only compensates the differences in magnitudes between major elements (e.g. Si or Al) and trace elements (e.g. the lanthanides or rare earth elements), but also it serves to make the distributions of geochemical data more nearly normal. In addition to that, the log-ratio transformation also detects possible perturbations in the chemical data because of contamination, diagenesis or other alteration processes (Buxeda i Garrigós and Kilikoglou, 2003; see Martin-Fernandez et al., 2015 for a thorough discussion on the use of log-ratio principles).

On the other hand, in order to test the variability that each chemical element and compound introduced into the dataset, the compositional heterogeneity was evaluated calculating the compositional variation matrix (MCV). Thus, when the variability is high (indicated by a large value of the total variation, vt), it suggests that the dataset is polygenic (i.e. presence of several compositional groups). On the contrary, a small vt value indicates a possible monogenic nature of the dataset (Buxeda i Garrigós and Kilikoglou, 2003).

2.1.2. X-Ray Diffraction (XRD)

A PANalytical X'pert PRO powder diffractometer was used for these analyses. For this, powdered ceramic pastes obtained following the procedure carried out by Sanchez-Garmendia and collaborators (2020) were used but calcination was not performed.

The instrument was equipped with a copper tube (λCuKαmean = 1.5418 Å), programmable divergence aperture, vertical goniometer (Bragg-Brentano geometry), automatic sample changer, PixCel detector and secondary graphite monochromator. The operating conditions for the Cu tube were 40 mA and 40 kV. The angular range (2 θ) was scanned between 5 º and 70 º. The treatment of the diffractogram data was carried out using X'pert HighScore (PANalytical) software in combination with the powder diffraction file database PDF2 (International Centre for Diffraction Data – ICDD, Pennsylvania, USA).

2.1.3. Scanning Electron Microscopy-Energy Dispersive Spectrometry (SEM-EDS)

The microstructural characterization and examination of the extent of vitrification, alterations and contaminations of the ceramics were analyzed using the EVO 40 Carl-Zeiss Scanning Electron Microscopy (SEM) coupled to an Energy Dispersive X-ray analyzer (EDS) X-Max. This study was conducted on 11 ceramic pieces after being transversally cut, embedded in epoxy resin, polished and gold coated, as well as in 5 freshly fractured surfaces that were cut perpendicularly to the outer/inner surfaces. The working conditions for SEM were the following: 20 kV, 100 mA, full vacuum conditions and 7.5-10.5 mm working distance. Then, for EDS the intensity is increased to 500 mA to improve the signal. The elemental composition of the ceramics was determined by an Energy Dispersive Spectrometry (EDS) analysis; the EDS spectra were acquired and treated using the INCA software.

3. Results and discussion

3.1. Identification of the compositional groups by the ICP-MS

The mean, minimum and maximum concentrations of each element and their average expanded uncertainties (U) as well as the relative standard deviation (RSD) for the 25 ceramics obtained by ICP-MS, are presented in Table 2. The expanded uncertainty of the results has been calculated following the Guide to the Expression of Uncertainty in Measurement (GUM) (Possolo, 2015) with k = 2, which is equivalent to a 95 % confidence level, as in Calparsoro (2019) and Sanchez-Garmendia and collaborators (2020), considering the whole analytical procedure. Average values were calculated with the expanded uncertainty of the concentrations corresponding to all ceramics. It should be highlighted that although 42 elements and compounds have been analysed, only the components shown in the following table were retained for next operations, and the rest were

363 removed due to their high uncertainty values (U > 38 %, in the case of Ni, Pb and
364 Sn) and to that P_2O_5 and Zn showed values below to the detection limit. Although
365 CaO shows an uncertainty value of 84 %, it was retained because it is an
366 important component for the distinction of the ceramics, since the clays contained
367 calcium in a greater or lesser degree (e.g. calcareous or low-calcareous
368 ceramics), depending on their source and the function that the ceramics were
369 going to have (Fabbri et al., 2014). The whole data set of the concentrations for
370 each element and ceramic and the standard deviations is presented in Table A.1
371 in the Appendix.

	Mean	Min	Max	RSD	$\overline{U}$ (%)
Al_2O_3	17.9	15.0	21.5	10	6.0
Ba	407	364	475	7	5.0
CaO	4.15	3.08	5.66	16	84
Ce	97.6	71.5	121	14	6.0
Co	29.4	16.0	88.6	51	26
Cr	44.5	22.9	74.8	27	38
Cs	26.3	20.7	32.5	11	4.0
Cu	12.2	3.00	37.1	74	24
Dy	5.25	3.84	6.70	14	13
Er	2.64	2.06	3.18	11	22
Eu	1.28	0.999	1.83	16	11
Fe_2O_3	5.01	3.68	7.62	19	8.0
Gd	6.35	4.90	8.06	14	10
Hf	6.23	5.05	8.18	11	6.0
Ho	0.751	0.577	0.946	13	20
K_2O	4.56	3.99	5.72	8	4.0
La	48.3	36.4	60.2	13	5.0
Lu	0.437	0.312	0.584	15	17
MgO	1.76	1.35	2.22	11	18
MnO	0.0208	0.0142	0.0348	24	28
Na_2O	0.606	0.365	1.11	28	34
Nb	20.5	15.4	25.4	13	4.0
Nd	41.6	30.8	52.7	15	6.0
Pr	11.0	8.32	13.6	15	5.0
Rb	302	252	362	8	3.0
SiO_2	73.7	66.8	83.5	5	5.0
Sm	7.53	5.40	10.1	17	6.0
Sr	89.9	74.6	125	11	19
Ta	3.03	2.33	3.70	13	8.0
Tb	0.855	0.614	1.12	15	8.0
Th	17.3	13.3	21.0	12	13
TiO_2	0.735	0.593	0.941	12	9.0
Tm	0.423	0.322	0.516	13	22
U	5.19	3.47	8.96	25	17
V	59.9	40.1	96.7	27	16
Yb	2.60	2.04	3.10	12	19

Zr	230	180	316	13	6.0

Table 2. Elemental concentrations, minimum and maximum values and their average expanded uncertainty (U) as well as the relative standard deviation (RSD) for the 25 ceramics obtained by ICP-MS. The RSD has been calculated using all the values of the same component in the 25 ceramics. The concentrations of the elements are expressed in ng/g, whereas for oxides in wt %.

The variability that each chemical element and compound introduced into the dataset was evaluated calculating the compositional variation matrix (MCV) (Figure 5). The y-axis (τ.i) represents the calculated value for the log-ratio variation for each element in the dataset. In this case, the set of 25 ceramics shows relatively medium-low vt (1.09) which reveals the high contribution of Cu, Co and Na_2O (Figure 5-A).

The analytical variance should be originated by natural sources. In contrast, experimental errors and/or alterations arising from post-depositional processes might increase it. Therefore, several elements were not considered for the statistical analyses in this work. Thus, on the one hand, as the tungsten carbide cell used to mill the ceramics is a potential contaminator, Co and Ta were removed. The reason is that Co is a known binder of tungsten alloys and usually occurs along with Ta traces (Boulanger et al., 2013). On the other hand, Na_2O was not considered because salt crystallization in porous materials, such as ceramics, is one of the primary causes of their deterioration, especially in marine environments (López-Arce et al., 2013). Likewise, Cu, the next most varying element, showed a high variability related to the post-depositional contaminations (Buxeda i Garrigós, 1999; Buxeda i Garrigós and Kilikoglou, 2003; Molera et al., 1993). For this reason, it was decided not to consider it for the statistical analyses. Finally, P_2O_5 and Zn were omitted since they showed values below the detection limit. Moreover, P_2O_5 should also be discarded in statistical routines due to its high variability and potential as a key-role compound in alteration processes in underground and underwater environments, because it could be retained by the ceramic body (Freestone et al., 1985; Lemoine and Picon, 1982; Maritan and Mazzoli, 2004; Pradell et al., 1996). Given all these considerations, the vt drops down to 0.38 when those components are omitted from the statistical study (Figure 5-B). Along these lines, the low vt obtained for this combined dataset including ceramics recovered in the shipwreck and in the city, suggests that the dataset is monogenic, that is, there is no presence of several compositional groups (Figure 5-B). This is demonstrated in the Hierarchical Cluster Analysis (HCA) performed in order to compare ceramics recovered in the shipwreck and ceramics recovered in the church and produced in Aveiro, in which all of them define a single compositional group A-1 (Figure 6). Three ceramics (AVR004, AVR019 and AVR020) are slightly different from the rest due to some differences in their chemical composition, but these are not so significant to discriminate these three ceramics from the rest.

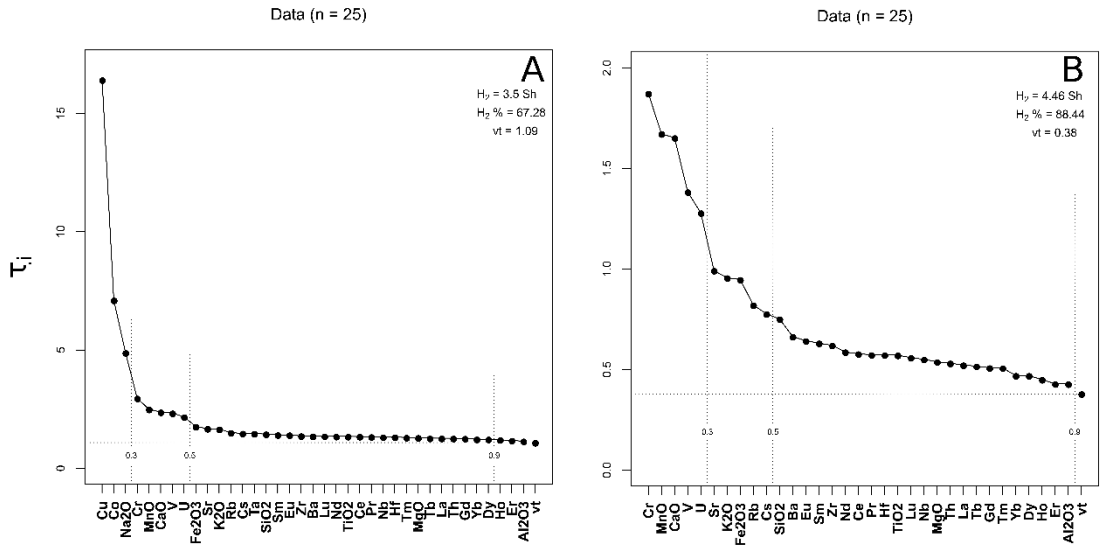

414

415 **Figure 5. A:** Graphical representation of the evenness of the compositional variability of
416 25 analyzed ceramics by ICP-MS. P_2O_5 and Zn were omitted since they showed values
417 below the detection limit and Ni, Pb and Sn because their high uncertainty values. // **B:**
418 Graphical representation of the evenness of the compositional variability of 25 analyzed
419 samples by ICP-MS, after excluding Co, Ta, Na_2O and Cu for the statistical analysis. (vt=
420 Total variability. H_2= information entropy, H_2%= percentage of information entropy over
421 the maximum possible, n= number of specimens (above)).

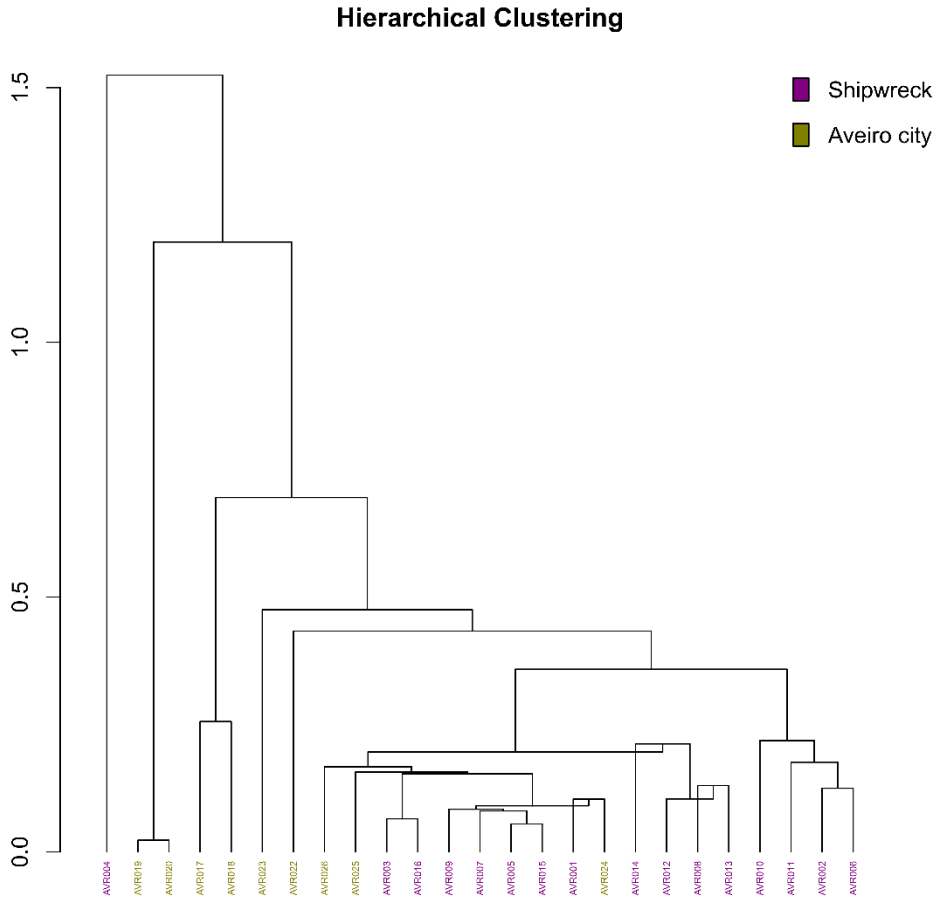

422

Figure 6. Dendrogram of Euclidean squared distances using centroid algorithm of 16 ceramics recovered in the shipwreck and 9 recovered in the church and produced in Aveiro, on the sub-composition of Al_2O_3, Ba, CaO, Ce, Cr, Cs, Dy, Er, Eu, Fe_2O_3, Gd, Hf, Ho, K_2O, La, Lu, MgO, MnO, Nb, Nd, Pr, Rb, SiO_2, Sm, Sr, Tb, Th, TiO_2, Tm, U, V, Yb, Zr.

Then, a HCA was performed to compare A-1 ceramics against several reference groups of productions of the Iberian Peninsula such as Seville, Zamora, Barcelona, Manises, Talavera, Nájera and some from Lisbon and Toro based on results obtained through ICP-MS, in order to test the possible exogenous provenances (Buxeda i Garrigós et al., 2015; Calparsoro et al., 2019; Iñañez et al., 2008; Iñañez et al., 2009; Sanchez-Garmendia et al., 2020) (Figure 7).

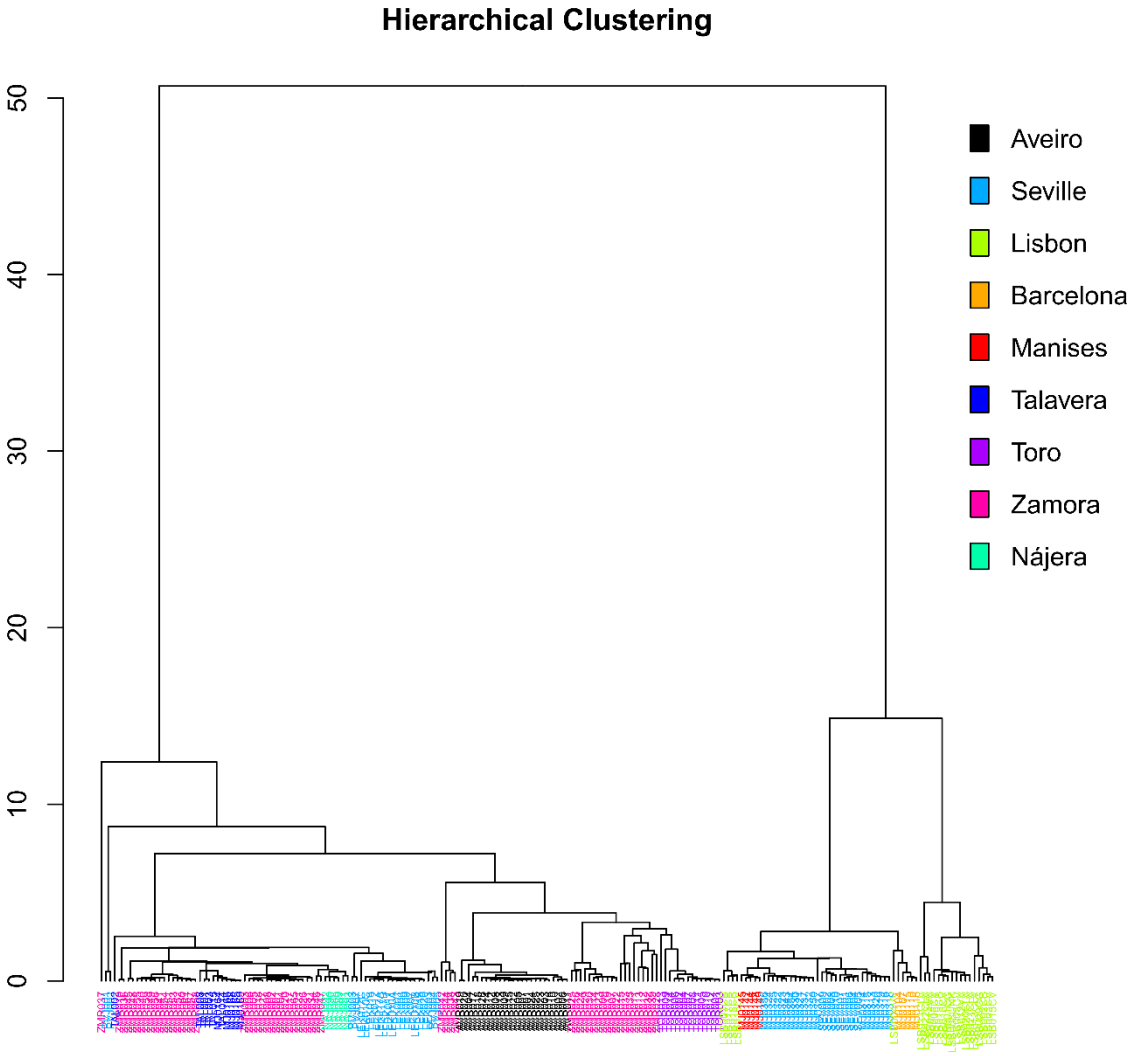

Figure 7. Dendrogram of Euclidean squared distances using centroid algorithm of 25 individuals from Aveiro (A-1 reference group) and different places from Iberian Peninsula, on the sub-composition of Al_2O_3, Ba, CaO, Ce, Cr, Cs, Dy, Er, Eu, Fe_2O_3, Gd, Hf, Ho, K_2O, La, Lu, MgO, Nb, Nd, Pr, SiO_2, Sm, Sr, Tb, Th, TiO2, Tm, V, Yb, Zr.

3.1.1. Provenance

Examination of the resulting dendrogram allows establishing a well-defined single group, named as A-1, structure that corresponds to the production of Aveiro, only

formed by ceramics unearthed in Ria de Aveiro A and in the dome of *Santo António* church. This fact is in accordance with the article published by Alves and collaborators (1998), which was explained in section 1. Regarding the main chemical features of this reference group, it can be said that it is a low-calcareous group, averaging 4.15 wt % of CaO. The forms dominating in this group are all unglazed olive jars, pots, cups, sugar moulds, plates and bowls, developing reddish and, in some cases, black pastes to visual appearance. The difference between the two sample sets (shipwreck and church) are those which could be seen in a macroscale: while the ceramics retrieved in the church have only red pastes and do not show shiny black surface and vitrified material, ceramics from the shipwreck show also black pastes and a shiny finish as well as some concretions or alterations in the paste.

3.2. Technological assessment by XRD

After identifying the compositional groups, XRD was conducted to identify the mineral phases and different production fabrics. A fabric is the final result that reaches the paste, after completing the technological process of the fabrication of the ceramics (Buxeda i Garrigós and Cau, 1995; Buxeda i Garrigós and Madrid i Fernández, 2016), which can be observed by the array of mineralogical composition and paste textures. In addition, the Firing Temperature (FT) in which the fabrics were fired was also evaluated.

The ceramics from Aveiro form five different production fabrics (F-I, F-II, F-III, F-IV and F-V) (Table 3). The main mineral phases of these four fabrics are quartz, potassium feldspars (principally microcline, sanidine and orthoclase) and plagioclases (principally albite and anorthite). The main differences between the fabrics are the existence or not of illite, hematites and hercynite, all depending on the firing temperatures and oxidizing/reducing conditions (Broekmans et al., 2008; Cianchetta et al., 2015; Nodari et al., 2004).

As regards the F-I group, it is completed with beige paste ceramics from RAVA and is divided in three subgroups: F-I_a, F-I_b and F-I_c (Table 3). The common phases are quartz, illite, potassium feldspars, hematite and plagioclases. On the other hand, the differences between these three groups are the amount of potassium feldspars, plagioclases, hematite and the appearance of secondary phases. It has to be highlighted that the ceramic that forms the F-I_a subgroup, is the only one that has a black matte surface in F-I. F-I_b seems to have more potassium feldspars and plagioclases than the rest, whereas the main difference between F-I_a, F-I_b and F-I_c is the amount of hematite: F-I_c has much more hematite than the others do. This fact could be related to the reduction of hematite in marine environments, suggesting that the iron of the hematite (Fe^{3+}) of F-I_a and F-I_b is lower because it was reduced to the iron of pyrite and/or jarosite (Fe^{2+}), whereas F-I_c did not suffer any or not too much hematite reducing reactions (see section 3.3) (Secco et al., 2011). This fact could be proven by the appearance of pyrite in the F-I_b fabric. Therefore, in the fabric F-I, the high presence of illite and the appearance of potassium feldspar allows establishing a Firing Temperature (FT) of 800 ºC (Figure 8).

The fabric F-II is formed by red paste ceramics and divided in two subgroups: F-II_a and F-II_b, completed by ceramics from RAVA and the church. The common phases are quartz, illite, plagioclases, potassium feldspars and hematite and the differences between these two subgroups is that F-II_a contains much more illite than F-II_b. Moreover, inside the group of F-II_a, ceramics from the church (AVR017 and AVR025) show more hematite than ceramics from RAVA (AVR013). This could be in accordance with the fact that in marine environment hematite could be reduced (Secco et. al., 2011). As illite is present but is decreasing in the amount, the FT of the fabric F-II is in the range of 800-850 ºC (Figure 8).

When it comes to the fabric F-III, formed by red ceramics from RAVA and the church, it presents quartz, potassium feldspars, plagioclase and hematite. As the no appearance of illite suggests its decomposition, the FT is of 900 ºC (Figure 8).

The F-IV fabric is formed by one black matte ceramic (surface and paste) from RAVA and it presents quartz, little illite, plagioclases, potassium feldspars and hercynite. There is no hematite, and this fact could suggest that the hematite could have been reduced to hercynite, in addition to the reductions that could happen in the marine environment (Broekmans et al., 2008; Cianchetta et al., 2015; Nodari et al., 2004). The total reduction of hematite could be explained by the black colour of AVR002 ceramic shard. In this fabric, the presence of a little amount of illite, potassium feldspar and hercynite permits establishing an FT in the range of 850-900 ºC (Figure 8).

Finally, F-V fabric, divided in two subgroups, is formed by four metallic shiny black surface ceramics from RAVA, showing quartz, potassium feldspars, plagioclases and hercynite. F-V_a is formed by a ceramic which shows a dark red paste, whereas F-V_b is formed by ceramics with black paste. The main difference between these two subfabrics is the appearance of hematite in F-V_a, suggesting that the reduction conditions were not fully achieved in AVR016 ceramic (see section 3.3). Additionally, some secondary phases in some shards, as well, were identified, like potassian halite (AVR003). According to literature, sodium-potassium chloride (potassium halite) was also detected in an Italic amphora recovered in an underwater marine environment (López-Arce et al., 2013). Given these conditions, the FT of this fabric is of 950 ºC. The amount of hercynite particularly draws the attention in F-V_b, because it is the highest peak in comparison with the rest of the fabrics (Figure 8).

Additionally, the white slip of AVR017 ceramic (olive jar) has been analyzed. The phases that are clearly differentiated are quartz, calcite and clay minerals (Figure 8). Thus, this slip was made mainly by a calcareous substrate likely mixed with clay to facilitate bonding to the ceramic surface while providing a white surface that covered the whole piece. However, the reason for applying such slip, beyond aesthetic features or for marking specific product containing the olive jar, remains unknown.

FT (ºC)	Fabrics	Ceramics	Subgroups	Typology	Qz	Ilt	Kfs	Pl	Hem	Hc	Py	Hl	Cal
800	F-I	AVR001	F-I_a	Beige paste	X	X	X	X	X				
		AVR004	F-I_b		X	X	X	X	X		X		
		AVR008, AVR009	F-I_c		X	X	X	X	X				
800 - 850	F-II	AVR013, AVR017, AVR025	F-II_a	Red paste	X	X	X	X	X				X (surface of AVR017)
		AVR006	F-II_b		x	x	x	x	x				
900	F-III	AVR007, AVR010, AVR011, AVR012, AVR014, AVR018, AVR019, AVR020, AVR022, AVR023, AVR024, AVR026	F-III	Red paste	X		X	X	X				
850 - 900	F-IV	AVR002	F-IV	Black paste and black matte surface	X	X	X	X		X			
950	F-V	AVR016	F-V_a	Dark red paste and black shiny surface	X		X	X	X	X			
		AVR003, AVR005, AVR015	F-V_b	Black paste and black shiny surface	X		X	X		X		X (AVR003)	

532

533 **Table 3.** The composition of each fabric and Summary of the results obtained by XRD (the FT,
534 subgroups, ceramics and typology and composition of each fabric). Qz= quartz; Ilt= illite; Kfs=
535 potassium feldspar; Pl= plagioclase; Hem= hematite; Hc= hercynite; Py= pyrite; Hl= potassium
536 halite; Cal= calcite, abbreviations according to Whitney and Evans (2010).

537

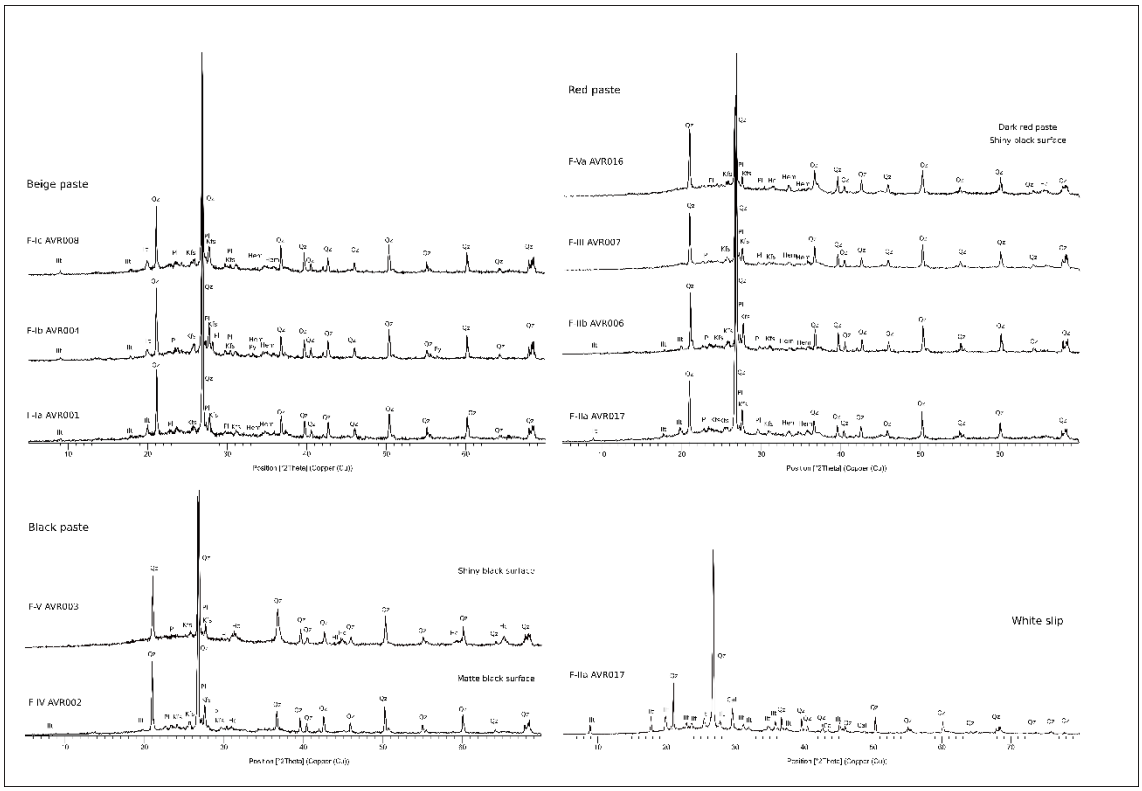

Figure 8. Reference diffractograms of the fabrics divided by the colour of the pastes (beige paste, red paste and black paste). Qz= quartz; Ilt= illite; Kfs= potassium feldspar; Pl= plagioclase; Hem= hematite; Hc= hercynite; Py= pyrite; Hl= potassium halite; Cal= calcite, abbreviations according to Whitney and Evans (2010).

3.2.1. Black ceramic production

The ICP-MS analyses allowed to know that the source of clay used for the manufacture of these 25 ceramics was the same. Additionally, as it could be noticed by XRD analyses, the pastes are not the same, so the only reason for this fact that one can think about, is the different technology (e.g. different atmosphere conditions during firing, different finishing) applied with a view to obtaining red and black pastes. According to literature, the black coloration of ancient ceramics was obtained mainly in three ways: using carbon, adding manganese oxides to the clays and reducing iron oxides in a reducing atmosphere, during firing (Edwards and Chalmers, 2005; Gillies and Urch, 1983). The first case (the use of carbon) is based on using clays naturally rich in organic material or to which carbonaceous material has been added. Then, they are fired in reducing conditions and carbon is formed. This gives the black colour to the ceramic (Gillies and Urch, 1983). The third case (firing in reducing conditions) is probably the oldest of all ceramic-decoration processes (Noll et al., 1975). When iron oxides are fired, their colour is affected by temperature, duration of heating and atmosphere (Shepard, 1976). In an oxidizing atmosphere, iron oxides are mainly in the form of hematite. However, in a reducing atmosphere, iron oxides form spinel phases, like hercynite ($FeO{\cdot}Al_2O_3$) and magnetite (Fe_3O_4), which are predominantly black (Longworth and Tite, 1979; Maggetti et al., 1981; Noll et al., 1975). One of the hypotheses of the black ceramics that form F-IV and F-V, is that they were fired in reducing conditions in order to get the black colour. This black colour could have been obtained due to the reduction of hematite (Fe_2O_3)

566 to hercynite, indicating strong reducing firing conditions (Ibarra, 2006; Nodari et
567 al., 2004).

568 According to archaeological evidence, it was common in Aveiro to produce these
569 black ceramics for the forms related to kitchen wares, like cooking pots (Carvalho
570 and Bettencourt, 2012; Fernandes and Castro, 2012; Ibarra, 2006). The reason
571 for doing this could have been the good qualities that the ceramics obtain in these
572 reducing firing conditions: the carbon element that is caught in the ceramic paste
573 during the process decreases the permeability of the paste, so that these shards
574 are suitable for retaining liquids. The same circumstances provide also better and
575 more hygienic food preservation because the dirt and bacteria are not able to
576 pierce in the pores, preventing the ceramic pastes, in this way, from the
577 reproduction of these microorganisms (Sempere, 1982). On the other hand, the
578 reduced wares are harder than the common wares, so that they are more
579 resistant in the use (Sempere, 1982).

580

581 ### 3.3. SEM-EDS assessment

582

583 Finally, ceramics of each fabric were selected to study them by SEM and SEM-
584 EDS in order to analyze the microstructure, the extent of vitrification, alterations
585 and contaminations.

586

587 #### 3.3.1. Extent of vitrification

588 Five freshly fractured surface ceramics were selected for SEM analysis, because
589 their SEM examination provides information about the internal morphology
590 developed during the original firing, the extent of vitrification and pore structure
591 (Maniatis and Tite, 1978). Among the selected ceramics, two are from F-I
592 (AVR008, AVR009), one from F-II (AVR017), one from F-IV (AVR002), and one
593 from F-V (AVR003) (Table 4). In this way, the results of SEM demonstrate that
594 the F-I and F-II fabrics show an early initial vitrification due to the appearance of
595 isolated smooth-surfaced areas, whereas the F-IV shows a medium vitrification
596 (Maniatis and Tite, 1978). Finally, the F-V shows a continuous vitrification,
597 because a continuous smooth vitrified layer is formed over the whole fracture
598 surface (Figure 9) (Maniatis and Tite, 1978). All these results are in accordance
599 with their FTs.

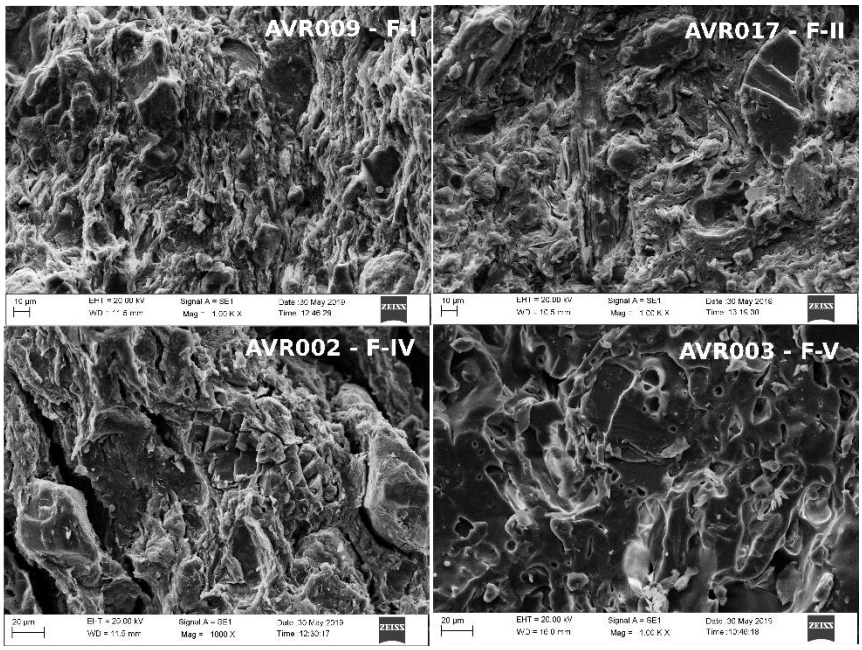

Figure 9. The grade of vitrification of **A)** F-I (ceramic AVR009), **B)** F-II (ceramic AVR017), **C)** F-IV (ceramic AVR002) and **D)** the grade of vitrification of F-V (AVR003).

Additionally, 11 transversally cut and polished pieces were selected for SEM-EDS analyses: 2 from F-I (AVR004, AVR008), 1 from F-II (AVR017), 4 from F-III (AVR007, AVR014, AVR016, AVR018) and 4 from F-V (AVR003, AVR005, AVR015, AVR016).

3.3.2. The glassy-layer

According to SEM-EDS results, none of the ceramics has any alkaline or tin-lead glaze, although a glassy-layer is observed in the shiny black ceramics from F-V (Figure 10). For the ceramics of F-V_b a glassy-layer that contains vacuoles could be observed, whereas for F-V_a (AVR016), the vacuoles are less abundant. The reason for the appearance of the glassy-layer could be that, at high temperatures, iron compounds may act as a flux when they are exposed to a reducing atmosphere, resulting in the change of the colour of the shard (from red to black) and also the formation of a glassy-layer in the surface (Rice, 2015). Additionally, Noll and colleagues (1975) explain that, for example, Cretan wares black painting was obtained reducing (by the iron reduction technique) iron-rich clays, which were added as a slip. The authors explain that in Cretan wares a high content of vacuoles were formed in the black paint layer. These vacuoles could have been formed due to the fact that during firing, some gases were formed in the form of bubbles (e.g. carbon dioxide) that attempt to escape through the layer. At higher temperatures, more of this glassy-layer is formed and the large number of bubbles/vacuoles could indicate a relatively high firing temperature (Noll et al., 1975). Thus, the existence of the vacuoles in the ceramics from Aveiro could be explained by the fact that Noll and collaborators report in their study. In these lines, a hypothesis is thought for AVR016 ceramic; it is from F-V_a subgroup, which shows a dark red paste and fewer vacuoles in the glassy-layer. Thus, this ceramic probably was red in origin but it was refired during the firing produced in the ship. As the firing environment around the ceramic cargo was probably a reducing environment (because they were covered), the hematite of the paste was reduced partially to hercynite, as it has been reported in section 3.2. Thus, the fewer

vacuoles of the glassy-layer and the partial reduction of hematite to hercynite could suggest that the interaction between the ceramic and the fire was not very strong when time exposed and temperature reached are considered. On the contrary, a strong interaction case could be the case of AVR005; this ceramic was probably red in origin, as well, but the reduction of hematite in this case was a total reduction. Moreover, the reason for thinking that AVR005 was red in origin, is that there is no archaeological evidence for black storage jars in Aveiro A excavation context. All storage jars recovered are red.

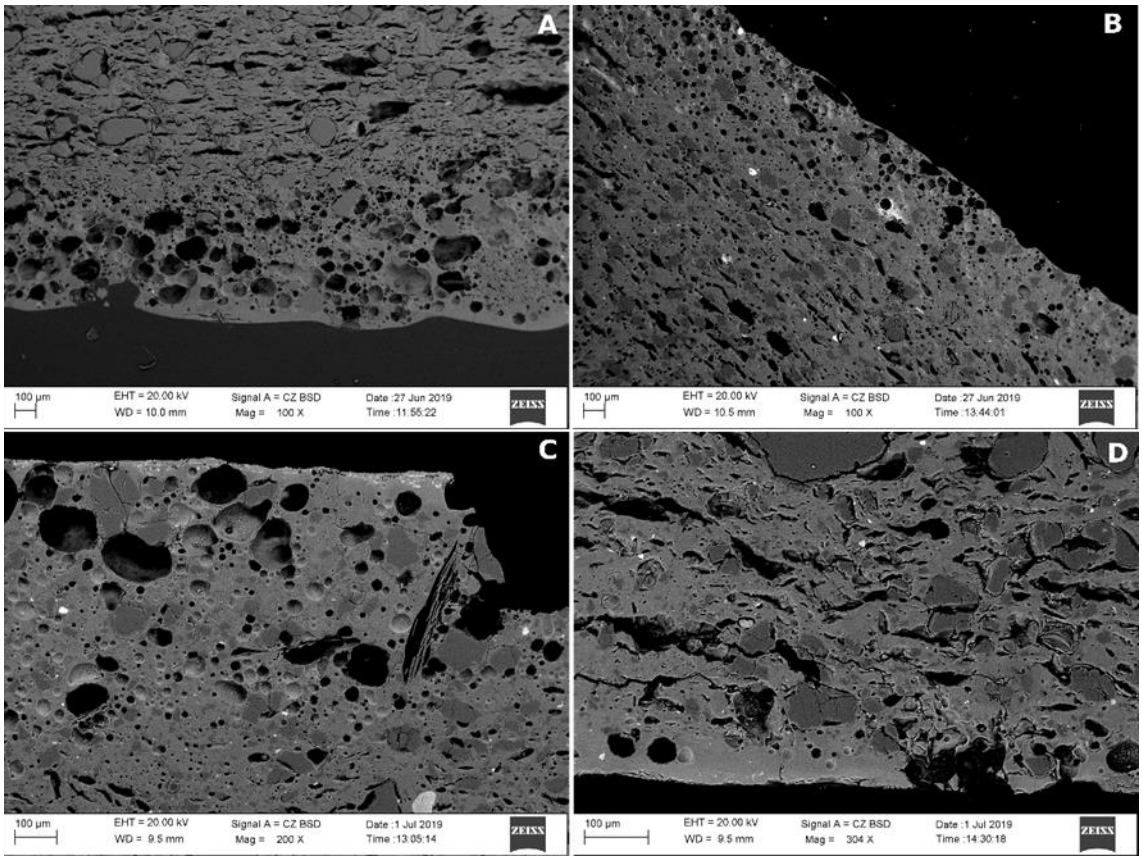

Figure 10. Four ceramic pieces from F-V showing a glassy-layer (**A:** AVR003, **B:** AVR005, **C:** AVR015 and **D:** AVR016).

3.3.3. The shiny black surface

The shiny black surface finishes found on ceramics studies here, have been applied in pottery from their earliest production. The reasons for applying them were both practical -because they provide more impermeable surface layer- and decorative (Tite et al., 1982). In some cases, the fine particle fraction of the body clay has been used to produce the black coating (in the case of Greek Attic black ceramics, for example) (Gillies and Urch, 1983). This is not the case of our ceramics, as no clay slip has been identified by SEM-EDS. In other cases, the metallic shiny black surface has been achieved by applying a burnished finishing in addition to the firing in high temperatures and reducing atmosphere. In this way, the shiny black surface is produced due to the alignment of the clay particles in the surface region on account of reducing firing conditions and burnishing (Gillies and Urch, 1983). According to Berg (2008), burnishing consists of the use of a hard, smooth object like wood, stone or bone, to rub the ceramic surface, often resulting in narrow parallel facets. By compressing the clay, burnishing

creates a characteristic luminous shine (Berg, 2008). Burnishing produces a uniform and compact surface, and it causes specular reflection, giving to the ceramics a “lustrous”, “shiny” or “glossy” surface like that obtained by different coatings (e.g. paints, slips, glazes). Contrariwise, smoothing makes ceramics appear “matte” or “dull” and this difference is because of different light reflections; the uniform surface allows for a large amount of light to be reflected directly back to the observer and thus the surface appears “lustrous” or “shiny” (Ionescu et al., 2014). This is the case for some black ceramics from Marginea (Romania) (Ionescu et al., 2014), Orsett (Essex, England) (Gillies and Urch, 1983), Indian “Northern Black Polished Ware” (Gillies and Urch, 1983) and Attic ceramics (Maniatis et al., 1993). Regarding the present case, burnished ceramics are well documented in Aveiro red and black ceramics, sometimes in vertical and crossed lines, creating geometric motifs in some of the closed forms (mugs, jugs/water jugs and storage jars) (Bettencourt and Carvalho, 2007-2008; Carvalho and Bettencourt, 2012). Additionally, Fernandes (2012) studies the black ceramic production from Portugal in her doctoral thesis and mentions that burnishing the surface of the pieces was, and still is, a technique widely used to decorate the surfaces of black or red pottery, leaving the surface shiny (Fernandes, 2012). Therefore, according to the literature presented, ceramics from F-V have been probably burnished because of the appearance of their shiny black surface.

3.3.4. Salt-glaze hypothesis

Additionally, the elements Na and Cl have been identified in an aggregate of AVR009, in the surfaces of AVR004 and AVR005 and in the ceramic body of AVR015 (Figure 11). Moreover, Na has been identified in the surface and body of some ceramics (AVR003, AVR004, AVR005, AVR006, AVR007, AVR008, AVR014, AVR015, AVR016) (Figure 11). Potassium halite has been identified as described in the section 3.2, as well. Although the sodium could be related to the sodium feldspars, especially in the ceramics that do not have a glassy-layer, the NaCl or Na could be related to the salt of the water environment from RAVA. Moreover, it could be related to the salt production and trade of Aveiro because fragments of a wood piece belonging to the shipwreck were discovered in the archaeological site of Ria de Aveiro A. By comparison with materials from other underwater contexts, it was recognized as a part of a shovel made of a single piece of log. It seems that the shovels were destined to load, unload and move the salt, although another function on board is not excluded. A similar shovel was also recovered in Newfoundland, associated with the conservation treatment of fish caught by European fishers who move there annually (Bettencourt and Carvalho, 2007-2008). Therefore, it could be thought that the ship was carrying salt in a location next to the ceramics or above them.

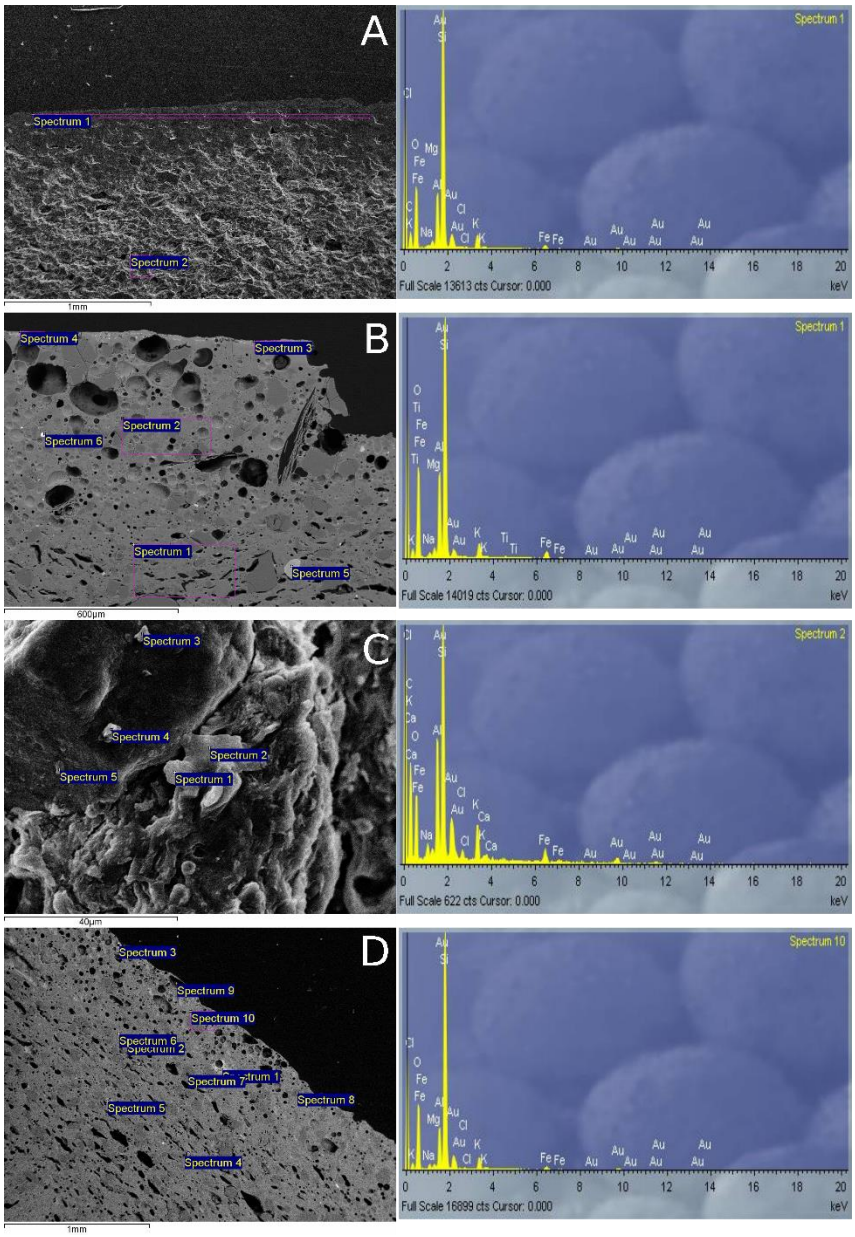

Figure 11. A: Na and Cl in the Surface of AVR004. B: Na in the body of AVR015. C: Na and Cl in an aggregate of AVR009. D: Na and Cl in the surface of AVR005.

As has been reported in section 1, several indications of a fire on board have been documented. In this context, it is possible to hypothesize about the presence of the salt and the fire on board. As the fire started in the ship, the salt could have reacted with the water in high temperatures (the temperatures of the fire), giving hydrogen chloride and sodium oxide (alkaline flux) as a product, according to the following reaction (Rice, 1987):

$$2NaCl + H_2O \rightarrow 2HCl\uparrow + Na_2O$$

The important role of the alkaline fluxes is to lower the very high melting point of silica, which is normally 1710 ºC (Rice, 1987). Therefore, this alkaline flux could have reacted with the silica of the pot surface ($Al_2O_3 \cdot 4SiO_2$), giving a glassy-layer as a product ($Na_2O \cdot Al_2O_3 \cdot 4SiO_2$):

$$Na_2O + Al_2O_3 \cdot 4SiO_2 = Na_2O \cdot Al_2O_3 \cdot 4SiO_2$$

These reactions can explain the presence of Na and not Cl in some ceramics and some concretions of some ceramics as well as the vacuolar aspect of the glassy-layers: the Cl was evaporated in the form of hydrogen chloride, leaving holes where before there were bubbles. This reaction and the formation of a glassy-layer also can be explained by the compositional difference of Na between the surface and the body of the ceramics that have the glassy-layer (Figure 12 and Table 4). These values demonstrate that the concentration of Na is higher in the surface than in the body, due to probably the formation of Na_2O in the surface. The difference in the concentration of Na also occurs in a lesser degree, that is, not with big differences, in other ceramics that do not have a glassy-layer (e.g. AVR014), but not in all of them (e.g. AVR004) (Figure 12 and Table 4). Moreover, this hypothesis can also explain the case of AVR005: the two ceramics that were next to each other in the ship could have reacted with the salt following the reaction explained, so that finally they got stuck.

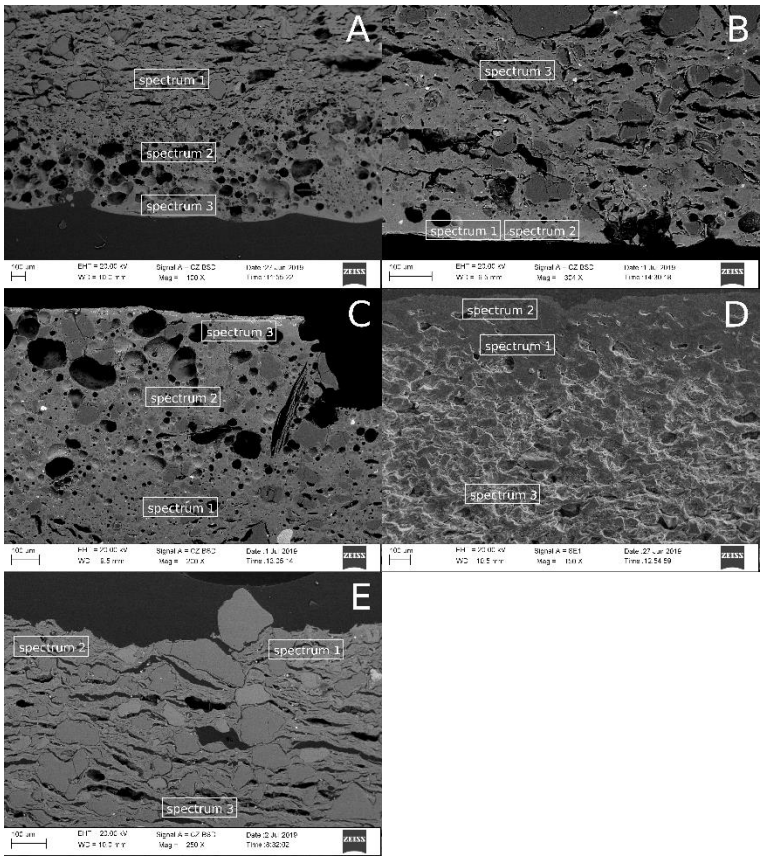

Figure 12. Elemental analyses in the different regions (surface, lower than the surface and body) of **A:** AVR003; **B:** AVR016; **C:** AVR015; **D:** AVR004 and **E:** AVR014, marked by the name of the spectrum.

ANID	Glassy-layer	Spectrum	Position	Na
A. AVR003	Yes	Spectrum 3	Surface	9,99
		Spectrum 2	Lower than the surface	1,97
		Spectrum 1	Body	0,29
B. AVR016	Yes	Spectrum 1	Surface	5,37

		Spectrum 2	Surface	6,03
		Spectrum 3	Body	0,64
C. AVR015	Yes	Spectrum 3	Surface	5,87
		Spectrum 2	Lower than the surface	2,79
		Spectrum 1	Body	0,77
D. AVR004	No	Spectrum 4	Surface	0,41
		Spectrum 3	Body	0,43
E. AVR014	No	Spectrum 1	Surface	0,39
		Spectrum 2	Surface	0,26
		Spectrum 3	Body	0,17

Table 4. Elemental concentrations of Na (in wt %) in different regions obtained by SEM-EDS of the ceramics shown in Figure 12.

3.3.5. Marine environments

Some aggregates composed by Fe, S, and in some cases, K have also been identified in the cavities and cracks of the ceramics (Figure 13).

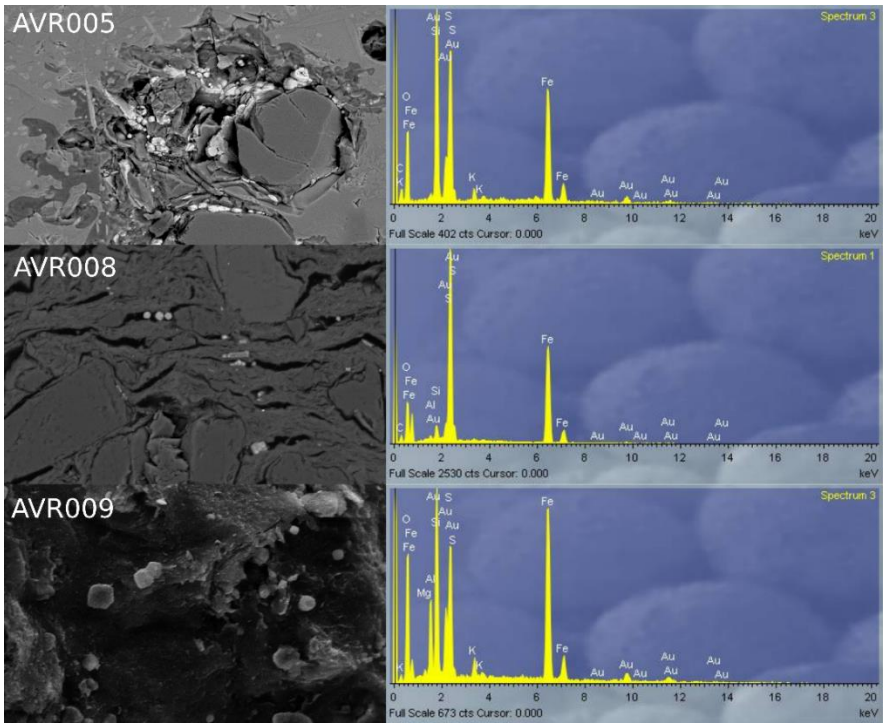

Figure 13. Aggregates in the cracks and cavities of AVR005, AVR008 and AVR009 composed mainly by Fe and S, and, sometimes, K.

According to the literature, these aggregates could be pyrite (FeS_2) and/or jarosite ($(K, Na)Fe_3(SO_4)_2(OH)_6$) (Secco et al., 2011). The presence of these two aggregates is a common alteration in marine environment ceramics, produced due to the decomposition of hematite (Fe_2O_3), from ferric ion (Fe^{3+}) to ferrous ion (Fe^{2+}), by the reduction and solubilization with hydrogen sulphide (H_2S) in water solution (Iñañez et al., 2020; Secco et al., 2011). In saline water environments, the microorganisms can reduce sulphate ions (SO_4^{2-}) to sulphur (S) or hydrogen sulphide, in the presence of sulphate-reducing bacteria (*Desulfovibrio desulfuricans*) (Neal et al., 2001; Secco et al., 2011). Then, this H_2S is the

responsible for hematite being reduced. Two main mechanisms could happen for this reduction, giving as a product framboidal aggregates or euhedral crystals of pyrite (Secco et al., 2011). On the one hand, hematite could hydroxilate to goethite (FeOOH), and subsequently, goethite could be reduced by H_2S to Fe^{2+}. On the other hand, hematite could be reduced directly to Fe^{2+} in the presence of H_2S. After these two reduction mechanisms, the ferrous ion reacts with additional hydrogen sulphide and forms pyrite as euhedral crystals or framboidal aggregates depending on the different sequences of reactions and the amount of organic matter and hydrogen sulphide (Neal et al., 2001; Schoonen, 2004; Secco et al., 2011). Then, jarosite could be formed due to the oxidation of pyrite and reaction with dissolved alkali (Secco et al., 2011).

4. Conclusions

This study provides a deeper understanding of pottery production and trade in Aveiro during the Post-Medieval period after the archaeometric characterization performed on 25 unglazed red and black low-calcareous ceramics unearthed in the archaeological site Ria de Aveiro A and the *Santo António* church. Thus, chemical analysis allowed stablishing their provenance as belonging to A-1 local reference group, which is related to the local pottery production of Aveiro during the 16th to the beginning of 17th centuries. These results are in accordance with the study carried out by Alves and collaborators (1998), which was explained in section 1.

As far as the manufacture technology is concerned, two main colours are distinguished among the pastes inside A-1 reference group: low-calcareous red and black, fired at temperatures ranging from 800 ºC to 950 ºC. Considering that all ceramics are formed with the same clays, the difference in the colour suggests that there is no specialization concerning the paste. Instead, in the first place, potters played with the temperature and the atmosphere of the kiln to obtain the colour of the paste they desired and, in the second place, they played with the different finishing of the ceramics. Thus, probably, they applied reducing conditions and high firing temperatures (850-950 ºC) for AVR002, AVR003 and AVR015 ceramics and this fact would be explained by the appearance of hercynite -after the reduction of hematite- in all of these ceramics. Echallier (1984) states that black pastes should therefore not be considered a priori as an indubitable index of technological poverty, but, on the contrary, as a conscious mastery of a simple and effective technique. However, two ceramics, which form the F-V fabric (AVR005 and AVR016), present a different case of study; probably, they were red ceramics in origin, however, the reducing firing conditions of the fire of the ship turned their surfaces to black. On the other hand, with respect to the shiny finishing of the ceramics, the potters probably burnished the shiny black shards of F-V fabric (AVR003, AVR005, AVR015 and AVR016), evidencing the burnishing technique in ceramics with red and black pastes (Fernandes, 2012). However, AVR002 from F-IV draws the attention because of its black matte surface. In order to obtain the metallic black finishing the potters used the technique of burnishing, as it produces an even and compact surface, which causes specular reflection and gives to the ceramics a shiny surface (Ionescu et al., 2014). Therefore, the reasons for this difference could be that, maybe they did not

give this finishing to AVR002 or that, AVR002 could have been smoothed instead of burnished because, according to the literature, smoothing makes ceramics appear matte (Ionescu et al., 2014).

Besides, SEM-EDS analyses have also facilitated the identification of the nature of a glassy-layer mainly of vacuolar aspect. One of the reasons for the formation of that layer is that iron compounds may act as a flux when they are exposed to a reducing atmosphere at high temperatures (Rice, 2015). In this case, the vacuoles could have been formed because of the gases (such as the carbon dioxide) formed during the original firing of high temperature or due to the fire produced in the ship. Therefore, the thickness of the glassy-layer would depend on the contact between the fire and the shards. On the other hand, the glassy-layer could have also been produced because of the reaction between the salt (NaCl) and the water. If the salt that was transported in the ship reacted with seawater (thanks to the high temperature of the fire), HCl and sodium oxide were formed according to the reaction of Rice (1987). Then, sodium oxide could have reacted with the silica of the ceramics, lowering its melting point, and giving as a product a glassy-layer. The vacuoles could be the product of the evaporation of HCl. Therefore, in this case, the thickness of the glassy-layer would depend on the amount of salt that reacted with the ceramics. The clear example would be the AVR005 ceramic, which has two ceramics stuck together: they were fused and melted together during the process. Furthermore, it is probably that the layers of the rest of the ceramics from F-V were also formed due to this reaction, as the higher concentration of Na in the surface of F-V ceramics suggested, probably due to the formation of Na_2O in the surface.

Moreover, the fire produced in the ship possibly did not act with the same intensity on all the shards, so some black spots may have appeared because the fire impacted directly on them (like in the case of AVR001, AVR012 or AVR013). Maybe, as with AVR005 and AVR016 happened, AVR002 was also burnt by the fire developed in the ship. Additionally, the beige surface of AVR003 could have been reoxidized during this process (Gillies and Urch, 1983).

In addition, XRD and SEM-EDS analyses have also shown the appearance of some secondary phases, such as pyrite or jarosite and evidences of potassium halite, related to alterations and contaminations of the ceramics in the post-depositional scenery. The presence of pyrite and jarosite aggregates is a common alteration in marine environment ceramics, produced due to the decomposition of hematite (Fe_2O_3), from ferric ion (Fe^{3+}) to ferrous ion (Fe^{2+}), by the reduction and solubilization with hydrogen sulphide (H_2S) in water solution (Secco et al., 2011). On the other hand, halite can crystallize in porous materials, especially in marine environments (López-Arce et al., 2013).

Finally, the present work reinforces the idea that local production from Aveiro, included in A-1 compositional group, clearly predominates in the city production pattern and was also a valuable object in the Atlantic trade. The fact that the ceramics from RAVA show a chemical fingerprint compatible with ceramics from the church, reinforce the conclusion of the study carried out by Carvalho and Bettencourt (2012); that ceramics from RAVA were from a latter period than it was thought, despite the ship being dated to the mid-15th century (Alves et al., 2001).

5. Acknowledgements

The ongoing investigation is framed in the research project *Archaeology and Archaeometry of the ceramic production and distribution in the Central-Northern Iberian Peninsula from the 16th to the 18th century* CERANOR-2 (HAR2017-84219-P), funded by the Spanish Ministry of Economy, Industry and Competitiveness, the State Bureau of Investigation, and the European Regional Development Fund (MINECO/AEI/ERDF, UE). USG thanks the University of the Basque Country (UPV/EHU) for doctoral grant Hiring for Research Training (PIF2017/153). JGI thanks the Spanish Ministry of Economy, Industry and Competitiveness for a Ramon y Cajal contract (RYC-2014-16835). The authors would like to thank Coupled Multispectroscopy Singular Laboratory (LASPEA) from the Advanced Research Facilities (SGIker) of The University of the Basque Country UPV/EHU) for SEM-EDS analysis. The authors also acknowledge The General X-ray Service from SGIker of the University of the Basque Country UPV/EHU as well as technical and human support provided by the SGIker-Geochronology and Isotope Geochemistry Facility (UPV/EHU, MICINN, GV/EJ, ERDF and ESF). Ria de Aveiro A shipwreck cargo excavation was made under the FCT project Rava 2000 (POCTI 34922/HAR/2000).

6. References

Aitchison, J., 1982. The statistical analysis of compositional data. J. R. Stat. Soc. Ser. B Methodol. 44, 2, 139-177.

Aitchison, J., 2008. The single principle of compositional data analysis, continuing fallacies, confusions and misunderstandings and some suggested remedies, in: CoDaWork, Girona. pp. 1-28.

Alves, F., Castro, F., Labrincha, J., 1998. Physical and chemical characterisation of archaeological ceramics found in a mid-15th century shipwreck in Ria de Aveiro, in Conference on Materials in Oceanic Environment (Euromat'98), Lisbon. 2, 223-232

Alves, F., Rodrigues, P., Aleluia, M., Rodrigo, R., Garcia, C., Rieth, E., Riccardi, E., 2001. Ria de aveiro A: A shipwreck from Portugal dating to the mid-15th century; a preliminary report. The International Journal of Nautical Archaeology. 30, 1, 12-36. doi: 10.1111/j.1095-9270.2001.tb01353.x.

Amorim, I., 2011. Sea Salt and Land Salt. The language of salt and technology transfer (Portugal since the Second Half of the 18th century), in: Marius Alexianu, Oliver Weller and Roxana-Gabriela Curcâ (Eds.), Archaeology and Anthropology of Salt: A Diachronic Approach. Proceedings of the International Colloquium, Cuza University. BAR S2198, 187-192.

Amorim, I., 2019. O comércio do sal de Aveiro na configuração de relações transfronteiriças do noroeste peninsular Ibérico (1692-1714), in: Manuel-Reyes García Hurtado (Eds.) Soltando amarras. La costa noratlántica ibérica en la Edad Moderna. A Coruña, Universidade da Coruña, 73- 101.

Antunes, C., 2008a. The commercial relationship between Amsterdam and the Portuguese Salt-Exporting Ports: Aveiro and Setúbal, 1580-1715, in: A articulação do sal português aos circuitos mundiais: antigos e novos consumos. Porto: Instituto de História Moderna - Universidade do Porto, 161-181.

Antunes, C., 2008b. The Commercial Relationship between Amsterdam and the Portuguese Salt-Exporting Ports: Aveiro and Setubal, 1580-1715. Journal of Early Modern History. 12, 25-53. 10.1163/138537808X297144.

Barbosa, T., Casimiro, T.M., Manaia, R., 2009. A late medieval household pottery group from Aveiro, Portugal. Medieval Ceramics, 30, 119-136.

Berg, I., 2008. Looking through pots: recent advances in ceramics X-radiography. Journal of Archaeological Science. 35, 5, 1177–88.

Bettencourt, J. and Carvalho, P., 2007-2008. A carga do navio Ria de Aveiro A (Ílhavo, Portugal): uma aproximaçao preliminar ao seu significado histórico-cultural. Cuadernos de estudios borjanos, 50-51, 257-287.

Bettencourt, J., 2009. Arqueologia marítima da Ria de Aveiro: uma revisão dos dados disponíveis, in: Octávio Lixa Filgueiras. Arquitecto de Culturas Marítimas. Lisboa, Âncora Editora, 137-160.

Boulanger, M.T., Fehrenbach, S.S., Glascock, M.D., 2013. Experimental evaluation of sample-extraction methods and the potential for contamination in ceramic specimens. Archaeometry. 55, 5, 880-892. https://doi.org/10.1111/j.1475-4754.2012.00706.x.

Broekmans, T., Adriaens, A., Pantos, E., 2008. Insights into the production technology of north-mesopotamian bronze age pottery. Appl Phys A. 90, 1, 35-42. doi: 10.1007/s00339-007-4227-y.

Buxeda i Garrigós, J. and Cau, M.A., 1995. Identificación y significado de la calcita secundaria en cerámicas arqueológicas. Complutum. 6, 293-309.

Buxeda i Garrigós, J., 1999. Alteration and Contamination of Archaeological Ceramics: The Perturbation Problem. J. Archaeol. Sci. 26, 3, 295-313. https://doi.org/10.1006/jasc.1998.0390.

Buxeda i Garrigós, J. and Kilikoglou, V., 2003. Total variation as a measure of variability in chemical data sets, in: van Zelst, L. (Ed.), Patterns and Process. A Festchrift in Honor to Dr. Edward Sayre. Smithsonian Center for Materials Research and Education, Suitland, Maryland, pp. 185-198.

Buxeda i Garrigós, J., Madrid i Fernández, M., Iñañez, J., Fernández de Marcos García, C., 2015. Archaeometry of the Technological change in societies in contact, in: Buxeda i Garrigós, J., Madrid i Fernández, M., Iñañez, J. (Eds.), Global Pottery 1. Historical Archaeology and Archaeometry for Societies in Contact. Archaeopress, Oxford, 3–26.

Buxeda i Garrigós, J. and Madrid i Fernández, M., 2016. Designing Rigorous Research: Integrating Science and Archaeology, in: The Oxford Handbook of Archaeological Ceramic Analysis. Oxford: Oxford University Press, pp. 19-47

Calparsoro, E., 2018. R Scripts for Reproducible Research on Archaeological Ceramics Compositional Data. https://doi.org/10.5281/zenodo.1411466.

Calparsoro, E., Sanchez-Garmendia, U., Arana, G., Maguregui, M., Iñañez, J.G., 2019. An archaeometric approach to the majolica pottery from alcazar of Nájera archaeological site. Herit. Sci. 7, 33. https://doi.org/10.1186/s40494-019-0275-9.

923 Calparsoro, E., 2019. Transdisciplinar methodologies on Medieval and Post-Medieval
924 pottery analysis: an archaeometric approach to Basque and Riojan Productions.
925 Doctoral Thesis.

926 Carvalho, P. and Bettencourt, J., 2012. De Aveiro para as margens do Atlântico: a carga
927 donavio Ria de Aveiro A e a circulação de cêramica na Época Moderna, In: Velhos e
928 Novos Mundos. Estudos de Arqueologia Moderna Old and New Worlds. Studies on Early
929 Modern Archaeology, Volume 2. Lisbon, 733-746

930 Carvalho, P., Bettenvourt, J., Coelho, I., 2014. The maritime cultural landscape of the ria
931 de aveiro lagoon (portugal) in the early modern period, in: Proceedings of the 5th
932 International Congress on Underwater Archaeology, Cartagena. 368-378.

933 Cianchetta, I., Trentelman, K., Maish, J., Saunders, D., Foran, B., Walton, M., Sciau, Ph.,
934 Wang, T., Pouyet, E., Cotte, M., Meirer, F., Liu, Y., Pianetta, P., Mehta, A., 2015.
935 Evidence for an unorthodox firing sequence employed by the berlin painter: Deciphering
936 ancient ceramic firing conditions through high-resolution material characterization and
937 replication. Journal of Analytical Atomic Spectrometry. 30, 3, 666-676. DOI:
938 10.1039/c4ja00376d.

939 Echallier, J.C., 1984. Éléments de technologie céramique et d'analyse des terres cuites
940 archéologiques. Documents d'Archéologie Méridionale, Serie Méthodes et Techniques,
941 3.

942 Edwards, H. G. M. and Chalmers, J. M., 2005. Raman spectroscopy in archaeology and
943 art history. Cambridge, UK: Royal Society of Chemistry.

944 Fabbri, B., Gualtieri, S., and Shoval, S., 2014. The presence of calcite in archeological
945 ceramics. Journal of the European Ceramic Society, 34, 7, 1899–1911.

946 Fernandes, I. M., 2012. A loiça preta em Portugal: Estudo histórico, modos de fazer e
947 de usar, in: Universidade do Minho.

948 Fernandes, I. M. and Castro, F., 2012. As produções de louça preta em Trás-os-Montes:
949 caracterização etnográfica e química; seu interesse para o estudo das cerâmicas
950 arqueológicas, In: Velhos e Novos Mundos. Estudos de Arqueologia Moderna Old and
951 New Worlds. Studies on Early Modern Archaeology, Volume 2. Lisbon, 975-982.

952 Freestone, I. C., Meeks, N. D., Middleton, A.P., 1985. Retention of phosphate in buried
953 ceramics: an electron microbeam approach. Archaeometry. 27, 2.
954 https://doi.org/10.1111/j.1475-4754.1985.tb00359.x.

955 García de Madinabeitia, S., Lorda, M.E., G. Ibarguchi, J.I., 2008. Simultaneous
956 determination of major to ultratrace elements in geological samples by fusion-dissolution
957 and inductively coupled plasma mass spectrometry techniques. Anal. Chim. Acta. 625,
958 2, 117-130. https://doi.org/10.1016/j.aca.2008.07.024.

959 Gillies, K. J. S. and Urch, D.S., 1983. Spectroscopic studies of iron and carbon in black
960 surfaced wares. Archaeometry. 25, 1, 29-44. doi: 10.1111/j.1475-4754.1983.tb00659.x.

961 Ibarra, J.L., 2006. Productos de alfarería negra posmedieval recuperados en contextos
962 arqueológicos de Vizcaya. Kobie (Serie Antropología Cultural). 12, 299-337.

963 Iñañez, J. G., Buxeda i Garrigós, J., Speakman, R.J., Glascock, M.D., 2008. Chemical
964 characterization of majolica pottery from the main production centers of the Iberian
965 Peninsula (14th-18th centuries). Journal of Archaeological Science. 35, 2, 425-440.

966 Iñañez, J. G., Speakman, R.J., Buxeda i Garrigós, J., Glascock, M.D., 2009. Chemical
967 characterization of tin-Lead glazed pottery from the Iberian Peninsula and the Canary
968 Islands: initial steps toward a better understanding of Spanish colonial pottery in the
969 Americas. Archaeometry. 51, 4, 546-567.

970 Iñañez, J. G., Bettencourt, J., Pinto, I., Teixeira, A., Arana, G., Castro, K., Sanchez-
971 Garmendia, U., 2020. Hit and sunk: provenance and alterations of ceramics from 17th
972 century Angra D shipwreck. Archaeological and Anthropological Sciences. (In Press).
973 doi: 10.1007/s12520-020-01109-y.

974 Ionescu, C., Hoeck, V., Crandell, O. N., Šarić, K., 2014. Burnishing versus smoothing in
975 ceramic surface finishing: A SEM study. Archaeometry. 57, 1, 18-26. doi:
976 10.1111/arcm.12089

977 Lemoine, C. and Picon, M., 1982. La fixation du phosphore par les céramiques lors de
978 leur enfouissements et ses incidences analytiques. Revue d'achéométrie. 6, 101-112.

979 Longworth, G. and Tite, M. S., 1979. Mössbauer studies on the nature of the red or black
980 glazes on Greek and Indian painted ware. Le Journal de Physique Colloques. 40, C2,
981 C2-461. doi: 10.1051/jphyscol:19792160.

982 López-Arce, P., Zornoza-Indart, A., Gomez-Villalba, L., Pérez-Monserrat, E. M., Álvarez
983 de Buergo, M., Vivar, G., Fort, R., 2013. Archaeological ceramic amphorae from
984 underwater marine environments: Influence of firing temperature on salt crystallization
985 decay. Journal of the European Ceramic Society. 33, 10, 2031-2042.
986 http://dx.doi.org/10.1016/j.jeurceramsoc.2013.03.009.

987 Maggetti, M., Galetti, G., Schwander, H., Picon, M., Wessicken, R., 1981. Campanian
988 pottery; the nature of the black coating. Archaeometry. 23, 2, 199-207. doi:
989 10.1111/j.1475-4754.1981.tb00306.x.

990 Maniatis, Y., Aloupi, E., Stalios, A. D., 1993. New evidence for the nature of the attic
991 black gloss. Archaeometry. 35, 1, 23-34. doi: 10.1111/j.1475-4754.1993.tb01021.x.

992 Maniatis Y. and Tite, M. S., 1978. Ceramic technology in the Aegean world during the
993 Bronze Age. Thera and the Aegean World. 1, 483-492.

994 Maritan, L. and Mazzoli, C., 2004. Phosphates in archaeological finds: implications for
995 environmental conditions of burial. Archaeometry. 46, 4, 673-683.
996 https://doi.org/10.1111/j.1475-4754.2004.00182.x.

997 Martín-Fernández, J., Buxeda i Garrigós, J., Pawlowsky-Glahn, V., 2015. Logratio
998 Analysis in Archeometry: Principles and Methods, in: Barceló, J.A., Bogdanovic, I. (Eds.),
999 Mathematics and Archaeology, CRC Press, Boca Raton, pp. 178-189.

1000 Molera, J., Pradell, T., Martínez Manent, S., Vendrell Saz, M., 1993. The growth of
1001 sanidine crystals in the lead of glazes of Hispano-Moresque pottery. Applied Clay
1002 Science. 7, 483-491. https://doi.org/10.1016/0169-1317(93)90017-U.

Morgado, P., Silva, R. C., Filipe, S., 2012. A cerâmica do açúcar de Aveiro: recentes achados na área do antigo bairro das olarias, in: Teixeira, A., Bettencourt, J. (Eds.), Velhos e novos mundos: estudos de arqueologia moderna. Lisboa, 2, 771–782.

Neal, A., Techkarnjanruk, S., Dohnalkova, A., McCready, D., Peyton, B., Geesey, G., 2001. Iron sulfides and sulfur species produced at hematite surfaces in the presence of sulfate-reducing bacteria. Geochimica et Cosmochimica Acta. 65, 223-235. DOI: 10.1016/S0016-7037(00)00537-8.

Newstead, S., 2014. Cod, Salt and Wine: Tracing Portuguese Pottery in the English North Atlantic World. North Atlantic Archaeology. 3, 75-92.

Nodari, L., Maritan, L., Mazzoli, C., Russo, U., 2004. Sandwich structures in the etruscan-padan type pottery. Applied Clay Science. 27, 1, 119-128. http://dx.doi.org/10.1016/j.clay.2004.03.003.

Noll, W., Holm, R., Born, L., 1975. Painting of ancient ceramics. Angewandte Chemie International Edition in English. 14, 9, 602-613. doi: 10.1002/anie.197506021

Possolo, A., 2015. Simple Guide for Evaluating and Expressing the Uncertainty of NIST Measurement Results. National Institute of Standards and Technology, 1297, 1–20. doi: 10.6028/NIST.TN.1900.

Pradell, T., Vendrell-Saz, M., Krumbein, W.E., Picon, M. 1996. Altérations de céramiques en milieu marin: les amphores de l'épave romaine de la Madrague de Giens (Var). Revue d'achéométrie. 20, 47-56.

Rice, P. M., 1987. Pottery analysis. Chicago [u.a.]: Univ. of Chicago Press.

Rice, P. M., 2015. Pottery analysis. A sourcebook, seconf edition. Chicago [u.a.]: Univ. of Chicago Press.

Sanchez-Garmendia, U., Calparsoro, E., Morillas, H., Arana, G., Iñañez, J. G., 2020. Pottery from the Ethnographic Museum archaeological site of Zamora: an archaeometric approach. Journal of Archaeological Sciencie Reports. (In press).

Schoonen, M. A. A., 2004. Mechanisms of sedimentary pyrite formation. Geological Society of America. 379, 117-134. DOI: 10.1130/0-8137-2379-5.117

Secco, M., Maritan, L., Mazzoli, C., Lampronti, G.I., Zorzi, F., Nodari, L., Russo, U., Mattioli, S.P., 2011. Alteration processes of pottery in lagoon-like environments. Archaeometry. 53, 809–829.

Sempere, E., 1982. Rutas a los alfares. Barcelona: Selbstverl.

Shepard, A. O., 1976. Ceramics for the archaeologist. 609. Repr. ed. Washington, DC: Carnegie Inst.

Silva, R. C., 2018. Um carrego de abóbada na igreja quinhentista de Santo António (Aveiro, Portugal). Revista portuguesa de arqueologia. 21, 1, 181-195.

Sousa, E., Silva, J., Gomes, C., 2005. Chemical and physical characterization of fragments from ceramic jars called "formas de açúcar" exhumed in the town of Machico, Madeira Island, in: Proceedings of the 7th European Meeting on Ancient Ceramics (EMAC'03).

1043 Tite, M. S., Freestone, I., Meeks, N., Bimson, M., (1982). The use of scanning electron
1044 microscopy in the technological examination of ancient ceramics. Smithsonian Institution
1045 Press, Washington D. C.

1046 Vieira, L. F., Ferreira, I., Ferraria, A. M., Casimiro, T. M., Colomban P., 2013. Portuguese
1047 tin-glazed earthenware from the 16th century: A spectroscopic characterization of
1048 pigments, glazes and pastes. Applied Surface Science. 285, 144-152. doi:
1049 10.1016/j.apsusc.2013.08.016.

1050 Weigand, P.C., Harbottle, G., Sayre, E.V., 1977. Turquoise sources and source analysis:
1051 Mesoamerica and the southwestern U.S.A., in: Exchange Systems in Prehistory,
1052 Academic Press, New York. pp. 15-34.

1053 Whitney DL, Evans BW, 2010. Abbreviations for names of rock-forming minerals. Am
1054 Miner. 95, 1, 185–7.